New genetic loci implicated in fasting glucose homeostasis and their impact on type 2 diabetes risk

Levels of circulating glucose are tightly regulated. To identify new loci influencing glycemic traits, we performed meta-analyses of 21 genome-wide association studies informative for fasting glucose, fasting insulin and indices of beta-cell function (HOMA-B) and insulin resistance (HOMA-IR) in up to 46,186 nondiabetic participants. Follow-up of 25 loci in up to 76,558 additional subjects identified 16 loci associated with fasting glucose and HOMA-B and two loci associated with fasting insulin and HOMA-IR. These include nine loci newly associated with fasting glucose (in or near *ADCY5*, *MADD*, *ADRA2A*, *CRY2*, *FADS1*, *GLIS3*, *SLC2A2*, *PROX1* and *C2CD4B*) and one influencing fasting insulin and HOMA-IR (near *IGF1*). We also demonstrated association of *ADCY5*, *PROX1*, *GCK*, *GCKR* and *DGKB-TMEM195* with type 2 diabetes. Within these loci, likely biological candidate genes influence signal transduction, cell proliferation, development, glucose-sensing and circadian regulation. Our results demonstrate that genetic studies of glycemic traits can identify type 2 diabetes risk loci, as well as loci containing gene variants that are associated with a modest elevation in glucose levels but are not associated with overt diabetes.

Impaired beta-cell function and insulin resistance are key determinants of type 2 diabetes (T2D). Hyperglycemia in the fasting state is one of the criteria that defines T2D[1], it can predict definitive clinical endpoints in nondiabetic individuals[2,3] and, when corrected in subjects with T2D, may help prevent microvascular[4,5] and long-term macrovascular[6,7] complications. To date, there are nearly 20 published loci reproducibly associated with T2D[8]; most of these are also associated with decreased insulin secretion[9] due to defective beta-cell function or beta-cell mass. Association studies for diabetes-related quantitative traits in participants without diabetes have also identified loci influencing fasting glucose levels, whose effects appear to be mediated by impairment of the glucose-sensing machinery in beta cells[10–17].

We recently formed the Meta-Analyses of Glucose and Insulin-related traits Consortium (MAGIC) to conduct large-scale meta-analyses of genome-wide data for continuous diabetes-related traits in participants without diabetes[15]. We aimed to identify additional loci that influence glycemic traits in individuals free of diabetes and investigate their impact on related metabolic phenotypes. We were also interested in understanding variation in the physiological range of glycemia and evaluating the extent to which the same variants influence pathological fasting glucose variation and T2D risk. The initial MAGIC collaboration identified the fasting glucose- and T2D-associated locus in *MTNR1B*[15], which was also reported by others[16,17]; this finding demonstrated that studies of continuous glycemic phenotypes in nondiabetic individuals can complement the genetic analyses of diabetes as a dichotomous trait and can improve our understanding of the mechanisms involved in beta-cell function and glucose homeostasis. Here, we extend our previous approach by performing meta-analyses of ~2.5 million directly genotyped or imputed autosomal SNPs from 21 genome-wide association studies (GWAS). These 21 cohorts include up to 46,186 nondiabetic participants of

European descent informative for fasting glucose and 20 GWAS including up to 38,238 nondiabetic individuals informative for fasting insulin, as well as the surrogate estimates of beta-cell function (HOMA-B) and insulin resistance (HOMA-IR) derived from fasting variables by homeostasis model assessment[18]. Follow-up of 25 lead SNPs in up to 76,558 additional individuals of European ancestry identified nine new genome-wide significant associations (empirically determined as $P < 5 \times 10^{-8}$)[19] with fasting glucose and one with fasting insulin and HOMA-IR. Five of these loci also demonstrated genome-wide significant evidence for association between the glucose-raising allele and T2D risk in up to 40,655 cases and 87,022 nondiabetic controls.

The wealth of loci newly discovered to be associated with fasting glucose and HOMA-B contrasts with the single new locus identified for fasting insulin and HOMA-IR and suggests that there is a different genetic architecture for beta-cell function and insulin resistance. Furthermore, our data support the hypothesis that not all loci that influence glycemia within the physiological range are also associated with pathological levels of glucose and T2D risk.

RESULTS

Genome-wide association meta-analysis of glycemic traits

We conducted a two-stage association study in individuals of European descent (Online Methods, **Supplementary Fig. 1** and **Supplementary Table 1a,b**). Because we sought to identify variants that influence fasting glucose in the unaffected population, hyperglycemia in the diabetic range exerts deleterious effects on beta-cell function[20,21] and treatment can confound glucose and insulin measurements, we excluded individuals with known diabetes, those on anti-diabetic treatment, and those with fasting glucose ≥7 mmol/l. We combined data from 21 stage 1 discovery GWAS for fasting glucose ($n = 46,186$) and 20 GWAS for fasting insulin ($n = 38,238$), HOMA-B ($n = 36,466$)

---

*A full list of authors and affiliations appears at the end of the paper.

Table 1 SNPs associated with fasting glucose-related or insulin-related traits at genome-wide significance levels

	Glucose/HOMA-B selected SNPs			Fasting glucose				HOMA-B			
SNP	Nearest gene(s)	Alleles (effect/other)	Freq	Discovery P	I^2 estimate (P)	Global P	Joint analysis n	Discovery P	I^2 estimate (P)	Global P	Joint analysis n
rs560887	*G6PC2*	C/T	0.70	4.4×10^{-75}	0.31 (0.18)	8.7×10^{-218}	119,169	2.0×10^{-28}	0.54 (0.01)	1.5×10^{-66}	94,839
rs10830963	*MTNR1B*	G/C	0.30	1.2×10^{-68}	0.00 (1.00)	5.8×10^{-175}	112,844	1.8×10^{-22}	0.45 (0.03)	2.7×10^{-43}	90,364
rs4607517	*GCK*	A/G	0.16	4.5×10^{-36}	0.19 (0.46)	6.5×10^{-92}	118,500	7.5×10^{-8}	0.36 (0.12)	1.8×10^{-16}	94,112
rs2191349	*DGKB-TMEM195*	T/G	0.52	7.8×10^{-17}	0.10 (0.68)	3.0×10^{-44}	122,743	5.4×10^{-11}	0.09 (0.71)	2.8×10^{-17}	98,372
rs780094	*GCKR*	C/T	0.62	2.5×10^{-12}	0.00 (1.00)	5.6×10^{-38}	118,032	0.25	0.32 (0.18)	3.2×10^{-4}	93,990
rs11708067	*ADCY5*	A/G	0.78	8.7×10^{-9}	0.04 (0.89)	7.1×10^{-22}	118,475	2.2×10^{-4}	0.37 (0.10)	2.5×10^{-12}	94,212
rs7944584	*MADD*	A/T	0.75	1.5×10^{-9}	0.00 (1.00)	2.0×10^{-18}	118,741	1.1×10^{-4}	0.16 (0.51)	3.5×10^{-5}	94,408
rs10885122	*ADRA2A*	G/T	0.87	8.4×10^{-11}	0.00 (1.00)	2.9×10^{-16}	118,410	3.7×10^{-6}	0.11 (0.66)	2.0×10^{-6}	94,128
rs174550	*FADS1*	T/C	0.64	1.5×10^{-8}	0.00 (1.00)	1.7×10^{-15}	118,908	4.5×10^{-5}	0.01 (0.99)	5.2×10^{-13}	94,536
rs11605924	*CRY2*	A/C	0.49	1.5×10^{-9}	0.00 (1.00)	1.0×10^{-14}	116,479	5.2×10^{-6}	0.03 (0.94)	3.2×10^{-5}	92,326
rs11920090	*SLC2A2*	T/A	0.87	1.9×10^{-6}	0.00 (1.00)	8.1×10^{-13}	119,024	1.4×10^{-4}	0.36 (0.11)	4.5×10^{-6}	94,629
rs7034200	*GLIS3*	A/C	0.49	1.2×10^{-4}	0.00 (1.00)	1.0×10^{-12}	106,250	1.9×10^{-6}	0.19 (0.46)	1.2×10^{-13}	83,759
rs340874	*PROX1*	C/T	0.52	7.1×10^{-8}	0.00 (1.00)	6.6×10^{-12}	116,882	3.7×10^{-5}	0.00 (1.00)	5.3×10^{-6}	92,942
rs11071657	*C2CD4B*	A/G	0.63	2.8×10^{-7}	0.00 (1.00)	3.6×10^{-8}	114,454	0.23	0.08 (0.73)	0.002	90,675
rs11558471	*SLC30A8*	A/G	0.68	2.6×10^{-11}	–	–	45,996	1.4×10^{-6}	–	–	36,283
rs4506565	*TCF7L2*	T/A	0.31	1.2×10^{-8}	–	–	46,181	1.4×10^{-6}	–	–	36,461
	Insulin/HOMA-IR selected SNPs			Fasting insulin				HOMA-IR			
rs780094	*GCKR*	C/T	0.62	1.1×10^{-4}	0.14 (0.57)	3.6×10^{-20}	96,126	9.9×10^{-7}	0.25 (0.32)	3.0×10^{-24}	94,636
rs35767	*IGF1*	G/A	0.85	1.0×10^{-7}	0.17 (0.50)	3.3×10^{-8}	94,590	7.8×10^{-8}	0.26 (0.28)	2.2×10^{-9}	93,141

Directly genotyped and imputed SNPs were tested for association with fasting glucose, fasting insulin and homeostasis model assessment of beta-cell function (HOMA-B) and insulin resistance (HOMA-IR). Twenty-one discovery cohorts with genome-wide data were meta-analyzed (stage 1 discovery), and 25 SNPs were promoted for replication of the same trait in a set of 33 additional cohorts with *in silico* ($n = 7$) or *de novo* ($n = 26$) genotype data ($n = 31$ for fasting insulin, HOMA-B and HOMA-IR; for stage 2 replication P values and effect sizes, see **Table 2**). A joint analysis was then performed (global). Heterogeneity in the discovery sample was assessed using the I^2 index[48]. Replication was not attempted for SNPs in two known T2D-associated genes (*SLC30A8* and *TCF7L2*) that achieved genome-wide significance for fasting glucose in stage 1. Freq denotes the allele frequency of the glucose-raising allele. n = sample size. Note that the previously reported *GCKR* SNP has associations with glucose-related and insulin-related traits.

and HOMA-IR ($n = 37,037$) and analyzed associations for ~2.5 million autosomal SNPs directly genotyped and imputed[22,23] from HapMap CEU sample data, assuming an additive genetic effect for each of the 4 traits.

Inverse variance-weighted meta-analyses revealed 12 independent loci associated with fasting glucose and/or HOMA-B at genome-wide significance levels (**Table 1**, **Supplementary Table 2** and **Supplementary Fig. 2a,b**). These included five newly discovered associations for loci in or near *ADCY5*, *MADD*, *ADRA2A*, *CRY2* and *FADS1* (**Table 1** and **Fig. 1a–j**), four previously reported fasting glucose-associated loci in or near *GCK*, *GCKR*, *G6PC2* and *MTNR1B*, the recently reported[24] locus in *DGKB-TMEM195*, and two loci in the T2D susceptibility genes *TCF7L2* (rs4506565, $r^2 = 0.92$ with the previously reported SNP rs7903146) and *SLC30A8* (rs11558471, $r^2 = 0.96$ with the previously reported SNP rs13266634). Seven additional loci had reproducible evidence for association with fasting glucose and/or HOMA-B across studies at the arbitrary summary threshold of $P < 2 \times 10^{-5}$, chosen to prioritize SNPs for follow-up (**Table 1** and **Supplementary Table 2**). After excluding SNPs within the four previously discovered genome-wide significant fasting glucose loci in *GCK*, *GCKR*, *G6PC2* and *MTNR1B*, we still observed an excess of small P values compared to the distribution expected under the null hypothesis (**Fig. 2a,b**), suggesting that some of these additional loci are likely to represent new fasting glucose– and/or HOMA-B–associated loci that merit additional investigation.

Stage 1 analyses of fasting insulin and HOMA-IR revealed no loci that reached genome-wide significance, but there were six loci with consistent evidence for association across study samples at $P < 2 \times 10^{-5}$ (**Table 1**, **Supplementary Table 2** and **Supplementary Fig. 2c,d**). Comparison of the observed P values with the distribution expected under the null hypothesis showed an excess of small P values that warrant further investigation (**Fig. 2c,d**).

Replication studies and global meta-analysis for 25 loci

We carried forward to stage 2 all independent loci with association to any of the four traits at $P < 2 \times 10^{-5}$; we did not include SNPs in the known T2D genes *TCF7L2* and *SLC30A8*, for which no further validation was sought (**Table 1** and **Supplementary Table 2**). We also included the nominally associated top SNP from a likely biological candidate (*IRS1*, $P = 10^{-4}$ for HOMA-IR) and a locus with P values that approached genome-wide significance in several stage 1 discovery cohorts (*PLXDC2-NEBL*), even though their overall stage 1 P values were $> 2 \times 10^{-5}$ (**Table 1** and **Supplementary Table 2**). In total, 25 loci were chosen for replication.

We directly genotyped 25 variants in 26 additional stage 2 studies with up to 63,850 nondiabetic participants of European ancestry for fasting glucose and 25 studies with up to 52,892 participants for fasting insulin, HOMA-IR and HOMA-B (**Supplementary Table 1b** and Online Methods). We also obtained *in silico* replication data for 12,708 additional individuals from seven studies for fasting glucose (9,372 participants and five studies for fasting insulin, HOMA-IR and HOMA-B), for a total of up to 76,558 individuals for fasting glucose and 62,264 for fasting insulin, HOMA-IR and HOMA-B in stage 2 association analyses.

Our combined stage 1 and 2 meta-analysis, including a total of up to 122,743 participants for fasting glucose (98,372 for fasting insulin, HOMA-IR and HOMA-B), established genome-wide significant associations for nine new loci for fasting glucose and/or HOMA-B (in or near *ADCY5*, *MADD*, *CRY2*, *ADRA2A*, *FADS1*, *PROX1*, *SLC2A2*, *GLIS3* and *C2CD4B*) and one for fasting insulin and HOMA-IR (upstream of *IGF1*) (**Table 1** and **Fig. 1a–j**). Here, we replicate the recently reported associations of the loci *DGKB-TMEM195* (with fasting glucose)[24] and *GCKR* (with fasting glucose, fasting insulin and HOMA-IR)[11,12,25] at levels that exceed the threshold for genome-wide significance. Loci that had previously achieved genome-wide significant associations with fasting glucose (*G6PC2*, *MTNR1B* and *GCK*) were also confirmed (**Table 1**).
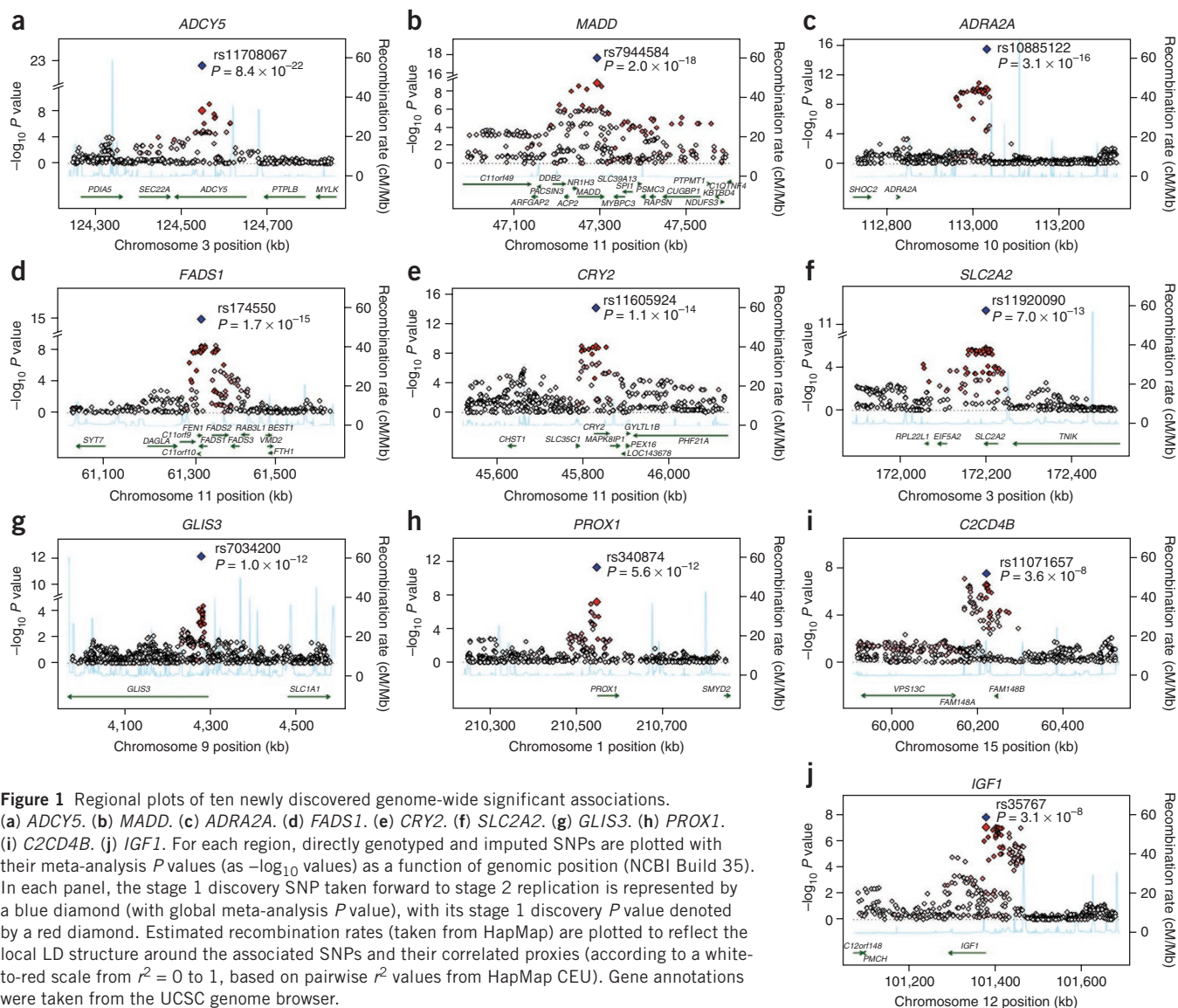
Figure 1 Regional plots of ten newly discovered genome-wide significant associations.
(**a**) *ADCY5*. (**b**) *MADD*. (**c**) *ADRA2A*. (**d**) *FADS1*. (**e**) *CRY2*. (**f**) *SLC2A2*. (**g**) *GLIS3*. (**h**) *PROX1*.
(**i**) *C2CD4B*. (**j**) *IGF1*. For each region, directly genotyped and imputed SNPs are plotted with
their meta-analysis P values (as $-\log_{10}$ values) as a function of genomic position (NCBI Build 35).
In each panel, the stage 1 discovery SNP taken forward to stage 2 replication is represented by
a blue diamond (with global meta-analysis P value), with its stage 1 discovery P value denoted
by a red diamond. Estimated recombination rates (taken from HapMap) are plotted to reflect the
local LD structure around the associated SNPs and their correlated proxies (according to a white-
to-red scale from $r^2 = 0$ to 1, based on pairwise r^2 values from HapMap CEU). Gene annotations
were taken from the UCSC genome browser.

We further conducted a global meta-analysis of cohort results
adjusted for body mass index (BMI) to test whether these diabetes-
related quantitative trait associations may be mediated by associations
with adiposity. The adjustment for BMI did not materially affect the
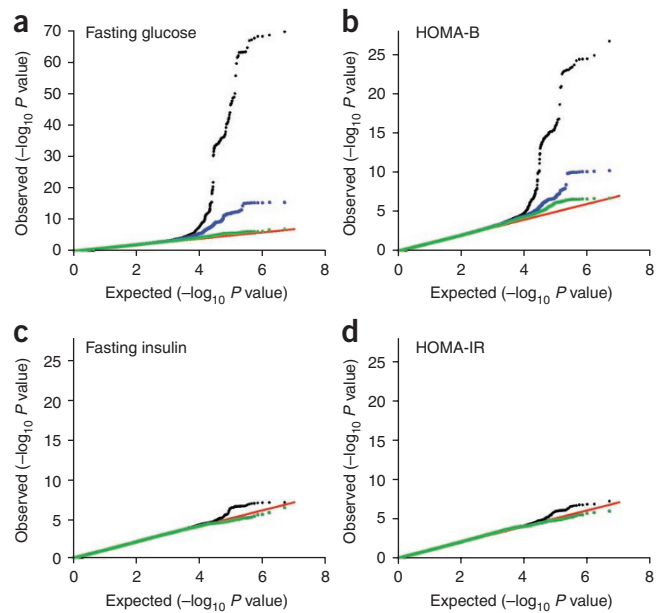strength of the associations with any of the traits (data not shown).

Effect size estimates for genome-wide significant loci
We restricted our effect size estimates (**Table 2** and **Supplementary
Table 2**) to the stage 2 replication samples (up to $n = 76,558$) to avoid
inflation introduced by the discovery cohorts (the so-called 'win-
ner's curse'[26]). The previously identified loci in *G6PC2*, *MTNR1B*
and *GCK* showed the largest effects on fasting glucose (0.075, 0.067
and 0.062 mmol/l per allele, respectively), with the remaining loci
examined showing smaller effects (0.008 to 0.030 mmol/l per allele;
Table 2). The proportion of variance in fasting glucose explained by
the 14 fasting glucose–associated loci with replication data (that is,
all fasting glucose loci except for those on *TCF7L2* and *SLC30A8*)
ranged from 3.2%–4.4% in the six replication studies providing this
information. Because results from our largest unselected commu-
nity-based cohort (Framingham) were on the lower bound of these

estimates (3.2%), we felt reassured that the winner's curse was not a
major concern in this instance and selected the Framingham cohort
to estimate the proportion of heritability explained and the geno-
type score. With a heritability estimate of 30.4% in the Framingham
cohort, these 14 loci explain a substantial proportion (~10%) of the
inherited variation in fasting glucose. Given the possibility that these
same loci harbor additional independent variants (for example, those
due to low-frequency alleles not captured by this analysis) that also
influence fasting glucose[27], this estimate of the heritability attribut-
able to these loci is likely to be conservative.

We estimated the combined impact of the 16 loci associated with
fasting glucose (the 14 loci included in the effect size estimates plus
those on *TCF7L2* and *SLC30A8*) in some of the largest cohorts
(Framingham, the Northern Finland Birth Cohort (NFBC) of 1966
and the Atherosclerosis Risk in Communities (ARIC) study) by con-
structing a genotype score equal to the sum of the expected number
of risk alleles at each SNP weighted by their effect sizes (see Online
Methods). Fasting glucose levels were higher in individuals with
higher genotype scores (**Fig. 3**), with mean differences of ~0.4 mmol/l
(5.93 versus 5.51 mmol/l in NFBC 1966; 5.36 versus 5.03 mmol/l in

Figure 2 Quantile-quantile plots. (**a**) Fasting glucose. (**b**) Beta-cell function by homeostasis model assessment (HOMA-B). (**c**) Fasting insulin. (**d**) Insulin resistance by homeostasis model assessment (HOMA-IR). In each plot, the expected null distribution is plotted along the red diagonal, the entire distribution of observed P values is plotted in black and a distribution that excludes the ten newly discovered loci shown in **Figure 1** is plotted in green. For fasting glucose and HOMA-B, the distribution that excludes the four genome-wide significant fasting glucose–associated loci reported previously (in *GCK*, *GCKR*, *G6PC2* and *MTNR1B*) is plotted in blue. A comparison of the observed P values for each trait shows that fasting glucose and HOMA-B associations are much more likely to be detected than fasting insulin and HOMA-IR associations.

Framingham; 5.70 versus 5.29 mmol/l in ARIC) when comparing individuals with a score of 23 or higher (5.6% of the sample) to those with a score of 12 or lower (2.9% of the sample). The 0.4 mmol/l (7.2 mg/dl) difference between the two tails of the distribution of risk score in the population (top 5.6% compared to the bottom 2.9%) is of clinical relevance, as it represents a shift of approximately 25 centile points in the distribution of fasting glucose. Prospective evidence has shown that a difference of this magnitude in fasting glucose is associated with a relative risk of 1.54–1.73 for future T2D, accounting for other risk factors[28]. The impact of individual SNPs on fasting glucose in the combined discovery and replication samples is shown in **Supplementary Figure 3**.

We also analyzed data from 1,602 self-reported white European children aged 5.9–17.2 from two studies. Though directionally consistent with observations in adults, some effect size estimates in these children were of smaller magnitude (data not shown). As in adults, the largest effect sizes were observed for risk alleles in *GCK* ($\beta = 0.085$, $P = 1.2 \times 10^{-5}$, $n = 1,602$), *G6PC2* ($\beta = 0.062$, $P = 1.9 \times 10^{-4}$, $n = 1,582$) and *MTNR1B* ($\beta = 0.033$, $P = 0.058$, $n = 1,309$).

Impact of reproducibly associated loci on additional glycemic traits
We sought to investigate all 17 loci associated with fasting glucose, HOMA-B, fasting insulin or HOMA-IR at genome-wide significance for their effects on other continuous glycemic traits. Whereas most of the 16 loci associated with fasting glucose are also strongly associated with HOMA-B (**Tables 1** and **2**), the associations between fasting glucose loci and fasting insulin were weak at best; *GCKR* is the only locus reaching genome-wide significant associations for both fasting glucose and fasting insulin or HOMA-IR, with the glucose-raising C allele being associated with increased fasting insulin (global $P = 3.6 \times 10^{-20}$) and HOMA-IR (global $P = 3.0 \times 10^{-24}$). These patterns are consistent with the gross trait correlations obtained in Framingham for fasting glucose and HOMA-B ($r = -0.43$) and for fasting glucose and fasting insulin ($r = 0.25$).

Impairment of glucose homeostasis may be characterized by elevated fasting glucose or fasting insulin, elevated glucose or insulin at 2 h after oral glucose tolerance test (OGTT), or elevated glycated hemoglobin (HbA_{1c}). We tested associations of each of the 17 loci of interest in a subset of MAGIC cohorts with GWAS data informative for these traits. Because HbA_{1c} is a measure of average glycemia over the preceding 2–3 months, we hypothesized that if an association of these loci with additional traits was present, it should be directionally consistent. The three loci with the largest effect sizes on fasting glucose—*G6PC2*, *MTNR1B* and *GCK*—all showed genome-wide significant and directionally consistent associations with HbA_{1c}; *DGKB-TMEM195*, *ADCY5*, *SLC2A2*, *PROX1*, *SLC30A8* and *TCF7L2* showed nominal ($P < 0.05$) evidence of directionally consistent association (**Table 2**). The fasting glucose–raising alleles at *TCF7L2*, *SLC30A8*, *GCK* and *ADCY5* were associated ($P < 0.0002$) with increased 2-h

glucose (**Table 2**); a parallel MAGIC project reports the genome-wide significant association with 2-h glucose of another *ADCY5* SNP in strong linkage disequilibrium (LD) with our lead SNP ($r^2 = 0.82$)[29]. In contrast, and consistent with previous reports that the fasting glucose–raising allele of *GCKR* is associated with greater insulin release during OGTT[11,12,30], this allele was associated with lower 2-h glucose.

Testing of these loci for association with T2D as a dichotomous trait in up to 40,655 cases and 87,022 nondiabetic controls demonstrated that the fasting glucose–raising alleles at seven loci (in or near *ADCY5*, *PROX1*, *GCK*, *GCKR* and *DGKB-TMEM195* and the known T2D genes *TCF7L2* and *SLC30A8*) are robustly associated ($P < 5 \times 10^{-8}$) with increased risk of T2D (**Table 2**). The association of a highly correlated SNP in *ADCY5* with T2D in partially overlapping samples is reported by our companion manuscript[29]. We found less significant T2D associations ($P < 5 \times 10^{-3}$) for variants in or near *CRY2*, *FADS1*, *GLIS3* and *C2CD4B* (**Table 2**). These data clearly show that loci with similar fasting glucose effect sizes may have very different T2D risk effects (see, for example, *ADCY5* and *MADD* in **Table 2**).

Given that several alleles associated with higher fasting glucose levels were also associated with increased T2D risk and that the T2D-related genes *TCF7L2* and *SLC30A8* showed association with fasting glucose, we systematically investigated association of all established T2D loci with the same four fasting diabetes–related quantitative traits. We found directionally consistent nominal associations ($P < 0.05$) of T2D risk alleles with higher fasting glucose for 11 of 18 established T2D loci, including *MTNR1B* (**Supplementary Table 3**). These data demonstrate that a large T2D effect size does not always translate to an equivalently large fasting glucose effect in nondiabetic persons, as clearly highlighted when contrasting the remarkably small effects of *TCF7L2* on fasting glucose compared to *MTNR1B* (**Table 2**).

Impact of new glycemic loci on other metabolic traits
Next, we used available GWAS results for additional metabolic phenotypes (BMI from GIANT[31], blood pressure from Global BPgen[32] and lipids from ENGAGE[33]) to assess the impact of the newly discovered glycemic loci on these traits. None of the newly discovered loci had significant ($P < 0.01$) associations with BMI or blood pressure (**Table 3**). Notably, the *FADS1* glucose-raising allele was associated with increased total cholesterol ($P = 2.5 \times 10^{-6}$),

Table 2 Association of newly discovered SNPs with glycemic traits in MAGIC and type 2 diabetes replication meta-analyses

SNP	Nearest gene(s)	Alleles (effect/other)		Fasting glucose (mmol/l)	HOMA-B	Fasting insulin (pmol/l)	HOMA-IR	HbA$_{1c}$ (%)	2-h glucose (mmol/l)	2-h insulin (pmol/l)	Type 2 diabetes[b]
rs560887	G6PC2	C/T	Effect[a]	0.075 (0.003)	–0.042 (0.004)	–0.007 (0.004)	0.006 (0.004)	0.032 (0.004)	0.017 (0.020)	–0.031 (0.013)	0.97 (0.95–0.99)
			P	8.5×10^{-122}	7.6×10^{-29}	0.11	0.16	1.0×10^{-17}	0.41	0.01	0.012
rs10830963	MTNR1B	G/C	Effect[a]	0.067 (0.003)	–0.034 (0.004)	–0.006 (0.004)	0.004 (0.004)	0.024 (0.004)	0.056 (0.022)	0.034 (0.015)	1.09 (1.06–1.12)
			P	1.1×10^{-102}	1.1×10^{-22}	0.14	0.37	3.0×10^{-9}	0.01	0.02	8.0×10^{-13}
rs4607517	GCK	A/G	Effect[a]	0.062 (0.004)	–0.025 (0.005)	0.004 (0.006)	0.015 (0.006)	0.041 (0.005)	0.097 (0.026)	–0.012 (0.015)	1.07 (1.05–1.10)
			P	1.2×10^{-44}	1.2×10^{-6}	0.46	0.01	6.3×10^{-19}	2.0×10^{-4}	0.42	5.0×10^{-8}
rs2191349	DGKB-TMEM195	T/G	Effect[a]	0.030 (0.003)	–0.017 (0.003)	–0.002 (0.003)	0.002 (0.004)	0.008 (0.003)	0.000 (0.019)	–0.006 (0.012)	1.06 (1.04–1.08)
			P	5.3×10^{-29}	6.4×10^{-8}	0.48	0.61	0.01	0.98	0.60	1.1×10^{-8}
rs780094	GCKR	C/T	Effect[a]	0.029 (0.003)	0.014 (0.003)	0.032 (0.004)	0.035 (0.004)	0.004 (0.004)	–0.091 (0.019)	0.000 (0.011)	1.06 (1.04–1.08)
			P	1.7×10^{-24}	1.4×10^{-5}	3.6×10^{-19}	5.0×10^{-20}	0.32	1.4×10^{-6}	1.00	1.3×10^{-9}
rs11708067	ADCY5	A/G	Effect[a]	0.027 (0.003)	–0.023 (0.004)	–0.011 (0.004)	–0.006 (0.005)	0.015 (0.004)	0.094 (0.023)	0.008 (0.015)	1.12 (1.09–1.15)
			P	1.7×10^{-14}	3.6×10^{-8}	0.01	0.16	5.1×10^{-4}	6.6×10^{-5}	0.60	9.9×10^{-21}
rs7944584	MADD	A/T	Effect[a]	0.021 (0.003)	–0.007 (0.004)	0.002 (0.004)	0.005 (0.004)	0.001 (0.004)	–0.017 (0.022)	–0.019 (0.013)	1.01 (0.99–1.03)
			P	5.1×10^{-11}	0.07	0.60	0.26	0.84	0.44	0.15	0.30
rs10885122	ADRA2A	G/T	Effect[a]	0.022 (0.004)	–0.010 (0.005)	0.001 (0.005)	0.004 (0.005)	0.007 (0.005)	0.004 (0.030)	–0.051 (0.019)	1.04 (1.01–1.07)
			P	9.7×10^{-8}	0.03	0.90	0.47	0.21	0.89	0.007	0.020
rs174550	FADS1	T/C	Effect[a]	0.017 (0.003)	–0.020 (0.003)	–0.011 (0.004)	–0.008 (0.004)	0.007 (0.004)	0.013 (0.019)	–0.003 (0.012)	1.04 (1.02–1.06)
			P	8.3×10^{-9}	5.3×10^{-10}	2.7×10^{-3}	0.03	0.053	0.49	0.82	2.3×10^{-4}
rs11605924	CRY2	A/C	Effect[a]	0.015 (0.003)	–0.005 (0.003)	0.001 (0.004)	0.003 (0.004)	0.001 (0.003)	0.023 (0.018)	0.006 (0.011)	1.04 (1.02–1.06)
			P	8.1×10^{-8}	0.13	0.73	0.34	0.72	0.20	0.62	1.7×10^{-4}
rs11920090	SLC2A2	T/A	Effect[a]	0.020 (0.004)	–0.012 (0.005)	0.002 (0.005)	0.005 (0.005)	0.017 (0.005)	0.015 (0.027)	–0.022 (0.016)	1.01 (0.99–1.04)
			P	3.3×10^{-6}	0.02	0.77	0.37	5.8×10^{-4}	0.58	0.19	0.34
rs7034200	GLIS3	A/C	Effect[a]	0.018 (0.003)	–0.020 (0.004)	–0.014 (0.004)	–0.011 (0.004)	0.003 (0.003)	0.037 (0.018)	0.010 (0.011)	1.03 (1.01–1.05)
			P	1.2×10^{-9}	8.9×10^{-9}	2.7×10^{-4}	4.6×10^{-3}	0.32	0.04	0.36	1.3×10^{-3}
rs340874	PROX1	C/T	Effect[a]	0.013 (0.003)	–0.008 (0.003)	–0.002 (0.004)	0.001 (0.004)	0.009 (0.004)	0.030 (0.020)	–0.007 (0.012)	1.07 (1.05–1.09)
			P	6.6×10^{-6}	0.02	0.68	0.74	9.5×10^{-3}	0.13	0.56	7.2×10^{-10}
rs11071657	C2CD4B	A/G	Effect[a]	0.008 (0.003)	–0.013 (0.004)	–0.009 (0.004)	–0.008 (0.004)	0.001 (0.004)	–0.065 (0.020)	–0.006 (0.013)	1.03 (1.01–1.05)
			P	0.01	8.1×10^{-4}	0.03	0.07	0.79	0.001	0.65	2.9×10^{-3}
rs13266634	SLC30A8	C/T	Effect[a]	0.027 (0.004)	–0.016 (0.004)	–0.004 (0.005)	–0.0002 (0.005)	0.016 (0.004)	0.093 (0.022)	–0.011 (0.015)	1.15 (1.10–1.21)[c]
			P	5.5×10^{-10}	2.4×10^{-5}	0.44	0.97	3.3×10^{-5}	2.0×10^{-5}	0.47	1.5×10^{-8}
rs7903146	TCF7L2	T/C	Effect[a]	0.023 (0.003)	–0.020 (0.004)	–0.012 (0.004)	–0.010 (0.004)	0.013 (0.003)	0.118 (0.021)	0.010 (0.013)	1.40 (1.34–1.46)[c]
			P	2.8×10^{-8}	1.4×10^{-7}	0.004	0.03	1.8×10^{-4}	2.6×10^{-8}	0.42	2.2×10^{-51}
rs35767	IGF1	G/A	Effect[a]	0.012 (0.005)	0.009 (0.005)	0.010 (0.006)	0.013 (0.006)	0.010 (0.005)	0.027 (0.025)	0.015 (0.016)	1.04 (1.01–1.07)
			P	0.01	0.09	0.10	0.04	0.050	0.28	0.33	6.6×10^{-3}
Sample size for each trait				45,049–76,558	35,435–61,907	37,199–62,264	35,901–62,001	33,718–44,856	15,221–15,234	7,051–7,062	40,655 cases/87,022 controls

[a]Per-allele effect (SE) for quantitative traits was estimated from stage 2 replication samples for fasting glucose, homeostasis model assessment of beta-cell function (HOMA-B), fasting insulin, and homeostasis model assessment of insulin resistance (HOMA-IR), and from discovery meta-analyses of MAGIC GWAS for glycated hemoglobin (HbA$_{1c}$), 2-h glucose after an oral glucose tolerance test (BMI-adjusted) and 2-h insulin (BMI-adjusted). For the first four traits, the regression coefficients are obtained from the replication cohorts so as to avoid an overestimate of the effect size caused by the 'winner's curse'. Results from replication samples were unavailable for rs7903146 and rs13266634; thus, discovery meta-analysis results are shown for both SNPs for fasting glucose ($n = 45,049–45,051$), HOMA-B ($n = 35,435–35,437$), fasting insulin ($n = 37,199–37,201$) and HOMA-IR ($n = 35,901–35,903$). [b]Replication genotyping was undertaken in 27 independent type 2 diabetes (T2D) case/control samples for all except the *TCF7L2* and *SLC30A8* signals. [c]Association with T2D for SNPs in *TCF7L2* and *SLC30A8* loci was estimated from the DIAGRAM+ meta-analysis for a total of 8,130 cases/38,987 controls. For these loci, we have included data on the most commonly associated SNPs with T2D in previously published data.

low-density lipoprotein cholesterol ($P = 8.5 \times 10^{-6}$) and high-density lipoprotein cholesterol ($P = 2.9 \times 10^{-5}$), but was associated with lower triglyceride levels ($P = 1.9 \times 10^{-6}$) (**Table 3**); a consistent association of this locus with lipid levels has been previously reported[34]. The fasting glucose–associated variant in *MADD* was not associated with lipid levels and is not in LD ($r^2 < 0.1$) with a previously reported high-density lipoprotein cholesterol SNP (rs7395662)[33], suggesting two independent signals within the same locus, one affecting lipid levels and the other affecting fasting glucose levels (**Table 3**).

Potential functional roles of newly discovered loci

We investigated the likely functional role of genes mapping closest to the lead SNPs using several sources of data, including human disease
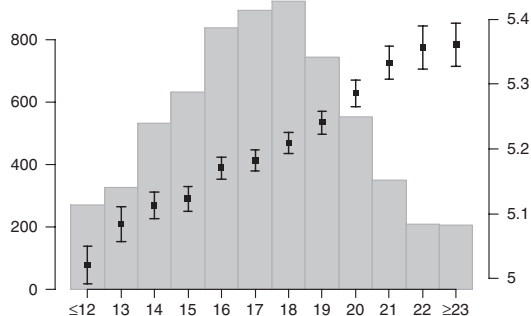

Figure 3 Variation in levels of fasting glucose depending on the number of risk alleles at newly identified loci, weighted by effect size in an aggregate genotype score for the Framingham Heart Study. The bar plots show the average and standard error of fasting glucose in mmol/l for each value of the genotype score based on the regression coefficient (right *y* axis), and the histogram denotes the number of individuals in each genotype score category (left *y* axis). Comparable results were obtained for the NFBC 1966 and ARIC cohorts. On average, the range spans ~0.4 mmol/l (~7.2 mg/dl) from low to high genotype score.

Table 3 Association of newly discovered SNPs with related metabolic traits in other GWAS datasets

SNP	Nearest gene(s)	Alleles (effect/other)		BMI (kg/m²)	Diastolic blood pressure (mm Hg)	Systolic blood pressure (mm Hg)	Hypertension	HDL	LDL	Total cholesterol	Triglycerides
rs560887	G6PC2	C/T	Effect[a]	−0.013 (0.010)	−0.146 (0.091)	−0.105 (0.135)	−0.023 (0.028)	−0.004 (0.004)	0.01 (0.011)	0.019 (0.011)	0.004 (0.005)
			P	0.18	0.12	0.46	0.41	0.32	0.35	0.10	0.52
rs10830963	MTNR1B	G/C	Effect[a]	0.002 (0.010)	0.034 (0.098)	0.088 (0.146)	−0.003 (0.030)	0.005 (0.004)	−0.015 (0.013)	0.002 (0.014)	−0.004 (0.007)
			P	0.86	0.74	0.56	0.91	0.26	0.25	0.88	0.58
rs4607517	GCK	A/G	Effect[a]	0.004 (0.011)	−0.136 (0.111)	−0.128 (0.165)	−0.013 (0.033)	−0.006 (0.005)	0.012 (0.014)	−0.002 (0.015)	0.013 (0.007)
			P	0.75	0.23	0.45	0.70	0.21	0.38	0.87	0.054
rs2191349	DGKB–TMEM195	T/G	Effect[a]	0.001 (0.009)	−0.075 (0.082)	−0.046 (0.122)	0.007 (0.025)	0.002 (0.003)	0.009 (0.01)	0.015 (0.011)	0.004 (0.005)
			P	0.95	0.37	0.71	0.79	0.64	0.40	0.18	0.44
rs780094	GCKR	C/T	Effect[a]	0.012 (0.009)	0.052 (0.084)	0.006 (0.124)	0.020 (0.025)	0.009 (0.003)	0.007 (0.01)	−0.019 (0.011)	−0.055 (0.005)
			P	0.17	0.55	0.96	0.45	8.7×10^{-3}	0.51	0.08	9.6×10^{-27}
rs11708067	ADCY5	A/G	Effect[a]	−0.010 (0.011)	−0.056 (0.104)	0.047 (0.156)	0.028 (0.031)	0.0004(0.004)	−0.014 (0.013)	−0.013 (0.013)	−0.003 (0.006)
			P	0.35	0.60	0.77	0.37	0.92	0.26	0.32	0.62
rs7944584	MADD	A/T	Effect[a]	0.023 (0.010)	−0.208 (0.093)	−0.170 (0.140)	−0.038 (0.028)	0.007 (0.004)	−0.013 (0.012)	−0.016 (0.012)	−0.007 (0.006)
			P	0.02	0.03	0.24	0.18	0.06	0.27	0.18	0.26
rs10885122	ADRA2A	G/T	Effect[a]	−0.021 (0.014)	−0.079 (0.131)	0.168 (0.193)	0.073 (0.039)	0.01 (0.007)	−0.019 (0.02)	−0.02 (0.021)	−0.02 (0.01)
			P	0.14	0.56	0.40	0.07	0.15	0.34	0.33	0.04
rs174550	FADS1	T/C	Effect[a]	0.003 (0.009)	−0.208 (0.086)	−0.108 (0.128)	0.013 (0.026)	0.014 (0.003)	0.046 (0.010)	0.052 (0.011)	−0.025 (0.005)
			P	0.73	0.02	0.42	0.62	2.9×10^{-5}	8.5×10^{-6}	2.5×10^{-6}	1.9×10^{-6}
rs11605924	CRY2	A/C	Effect[a]	0.011 (0.009)	0.123 (0.082)	−0.003 (0.123)	0.004 (0.025)	0.005 (0.004)	0.005 (0.011)	0.008 (0.011)	−0.009 (0.005)
			P	0.21	0.15	0.98	0.87	0.13	0.62	0.46	0.10
rs11920090	SLC2A2	T/A	Effect[a]	0.010 (0.012)	−0.034 (0.117)	−0.023 (0.174)	−0.030 (0.036)	0.003 (0.005)	−0.004 (0.014)	−0.009 (0.015)	−0.015 (0.007)
			P	0.42	0.78	0.90	0.41	0.60	0.81	0.57	0.04
rs7034200	GLIS3	A/C	Effect[a]	−0.002 (0.009)	0.093 (0.082)	0.087 (0.122)	0.006 (0.025)	0.0002(0.003)	0.015 (0.01)	0.028 (0.011)	0.005 (0.005)
			P	0.86	0.27	0.49	0.80	0.94	0.15	8.3×10^{-3}	0.37
rs340874	PROX1	C/T	Effect[a]	−0.007 (0.009)	0.113 (0.085)	0.093 (0.127)	0.029 (0.026)	−0.007 (0.003)	0.009 (0.01)	0.003 (0.011)	0.007 (0.005)
			P	0.46	0.20	0.48	0.27	0.04	0.39	0.81	0.19
rs11071657	C2CD4B	A/G	Effect[a]	−0.006 (0.010)	0.132 (0.091)	−0.007 (0.135)	0.020 (0.028)	−0.004 (0.004)	0.012 (0.011)	0.002 (0.011)	0.006 (0.005)
			P	0.54	0.16	0.96	0.49	0.22	0.28	0.86	0.30
rs13266634	SLC30A8	C/T	Effect[a]	−0.026 (0.011)	−0.081 (0.094)	−0.072 (0.139)	0.010 (0.029)	0.003 (0.004)	0.016 (0.011)	0.013 (0.011)	0.005 (0.005)
			P	0.01	0.40	0.62	0.74	0.47	0.13	0.24	0.33
rs7903146	TCF7L2	T/C	Effect[a]	−0.033 (0.009)	0.026 (0.091)	0.025 (0.137)	0.003 (0.028)	0.005 (0.004)	0.007 (0.012)	0.007 (0.012)	−0.006 (0.006)
			P	4.4×10^{-4}	0.78	0.86	0.92	0.22	0.53	0.55	0.31
rs35767	IGF1	G/A	Effect[a]	0.003 (0.012)	−0.102 (0.113)	−0.078 (0.167)	−0.005 (0.034)	0.003 (0.005)	−0.009 (0.015)	−0.012 (0.015)	−0.002 (0.007)
			P	0.81	0.38	0.65	0.87	0.56	0.52	0.43	0.84
			n	28,225–32,530	28,591–34,130	28,557–34,135	8,145–9,553 cases 8,175–9,749 controls	21,045	17,521	17,529	21,104

[a]Per-allele effect (s.e.m.). Results for BMI, blood pressure traits and lipid levels were kindly provided by the GIANT[31], GlobalBPGen[32] and ENGAGE[33] consortia, respectively.

databases, evidence from animal models and bioinformatic analyses (see Box 1, Online Methods and **Supplementary Table 4**). The newly discovered and previously established glycemic loci represent various biological functions: signal transduction (*DGKB-TMEM195*, *ADCY5, FADS1, ADRA2A, SLC2A2, GCK, GCKR, G6PC2* and *IGF1*), cell proliferation and development (*GLIS3, MADD* and *PROX1*), glucose transport and sensing (*SLC2A2, GCK, GCKR* and *G6PC2*) and circadian rhythm regulation (*MTNR1B* and *CRY2*). All of these pathways represent further avenues for physiological characterization and possible therapeutic intervention for T2D. However, we note that other genes could be causal (**Box 1** and **Supplementary Table 4**), and further experimental evidence will be needed to unequivocally link specific genes with phenotypes.

Expression analyses

We measured expression of the genes mapping closest to our lead SNPs (in *DGKB-TMEM195, ADCY5, MADD*, its neighboring gene *SLC39A13* (a member of a family of zinc transporters mapping ~45 kb from the *MADD* lead SNP), *ADRA2A, FADS1, CRY2, SLC2A2, GLIS3, PROX1* and *C2CD4B*) in human pancreas and other metabolically relevant tissues (**Supplementary Fig. 4a**). Although there was evidence of expression in human islets for nearly all genes tested (with the sole exception of *TMEM195*), we found that *DGKB* and *MADD* were

most strongly expressed in brain, *SLC2A2, FADS1, TMEM195* and *PROX1* were most strongly expressed in liver and *ADCY5* was most strongly expressed in heart, whereas *SLC39A13, ADRA2A* and *CRY2* were broadly expressed. Notably, *C2CD4B* was highly expressed in the whole pancreas with lower levels in isolated islets, suggesting that it is also present in exocrine cells. A duplicate experiment in a different laboratory obtained similar results (**Supplementary Fig. 4b**). We further examined expression of these transcripts in flow-sorted human beta cells from two separate individuals and documented beta-cell expression for all but *TMEM195*, with *SLC39A13, CRY2, GLIS3* and *PROX1* being particularly highly expressed in these cells (**Supplementary Fig. 4c**). Expression levels in metabolically relevant tissues for *DGKB* (beta cells) and *TMEM195* (liver) provided equally credible evidence for their respective candidacies as the causal gene at these loci. Furthermore, based on its relatively high expression levels in beta cells, *SLC39A13* (neighboring gene to *MADD)* constitutes a possible candidate gene that may merit further investigation.

Potential causal variants, eQTLs and copy number variants

Our results interrogate only a fraction of the common variants in any given genomic region; we therefore expect that for the majority of the loci here described, the underlying causal variant has yet to be identified. Nevertheless, for some loci there are possible SNP

Box 1: Genes nearest to loci associated with fasting diabetes-related quantitative traits

The **DGKB-TMEM195** locus was recently reported to be associated with fasting glucose[24]; here we report genome-wide significant replication of that finding and evaluate the genes mapping closest to the lead SNP in further detail. *DGKB* encodes the β (1 of 10) isotype of the catalytic domain of diacylglycerol kinase, which regulates the intracellular concentration of the second messenger diacylglycerol. In rat pancreatic islets, glucose increases diacylglycerol[49], which activates protein kinase C (PKC) and thus potentiates insulin secretion[50]. *TMEM195* encodes transmembrane protein 195, an integral membrane phosphoprotein highly expressed in liver.

ADCY5 encodes adenylate cyclase 5, which catalyzes the generation of cAMP. Upon binding to its receptor in pancreatic beta cells, glucagon-like peptide 1 (GLP-1) induces cAMP-mediated activation of protein kinase A, transcription of the proinsulin gene and stimulation of insulin secretory processes[51].

MADD encodes mitogen-activated protein kinase (MAPK) activating death domain, an adaptor protein that interacts with the tumor necrosis factor α receptor to activate MAPK. Both PKC and MAPK have been implicated in the proliferation of beta cells induced by GLP-1 (ref. 51), suggesting that *DGKB* and *MADD* may contribute to beta-cell mass and insulin secretion in this manner as well. Also in this region, **SLC39A13** encodes a putative zinc transporter required for connective tissue development and BMP/TGF-β signaling[52]. **NR1H3** encodes the liver X receptor alpha (LXRA) protein, which contains the retinoid response element. Glucose stimulates the transcriptional activity of LXR, which acts as a molecular switch that integrates hepatic glucose metabolism and fatty acid synthesis[53].

ADRA2A encodes the $α_{2A}$ adrenergic receptor, which is expressed in beta cells and whose activation leads to an outward potassium current independent of the islet potassium-sensitive ATP (K_{ATP}) channel, thus possibly modifying insulin release[54]. Mice with null mutations display abnormal glucose homeostasis in addition to cardiac hypertrophy and abnormal heart rate and blood pressure.

FADS1 encodes fatty acid desaturase 1, which catalyzes the biosynthesis of highly unsaturated fatty acids from precursor essential polyunsaturated fatty acids. One such product is arachidonic acid; in rodent beta cells, arachidonic acid liberated by phospholipase A_2 augments glucose-mediated insulin release[55]. Two other members of the same family, **FADS2** and **FADS3**, also reside in this region. By directing fatty acids down this metabolic pathway, increased activity of these enzymes may lower circulating triglyceride concentrations.

CRY2 encodes cryptochrome 2, an integral component of the mammalian circadian pacemaker[56]. Mice with null mutations in this gene present with abnormal circadian rhythmicity and several metabolic abnormalities including impaired glucose tolerance, increased insulin sensitivity, decreased body weight and adipose tissue, and abnormal heart rate. Together with **MTNR1B**[15–17], this is the second circadian gene associated with fasting glucose in humans, contributing further evidence to the emerging idea that this pathway regulates glucose homeostasis[57]. In the same region, **MAPK8IP1** encodes the scaffolding protein JIP1. Cross-talk between JIP1 and JIP3 has been implicated in the regulation of ASK1-SEK1-JNK signaling during glucose deprivation[58]. A missense mutation in this gene (leading to a S59N amino acid substitution) segregates with diabetes in one family affected with a Mendelian form of the disease[59].

SLC2A2 encodes the GLUT2 transporter responsible for transporting glucose into beta cells and triggering the glucose-mediated insulin secretion cascade. In humans, recessive mutations in this gene lead to Fanconi-Bickel syndrome, a rare disorder characterized by hepatorenal glycogen accumulation, proximal renal tubular dysfunction and impaired utilization of glucose and galactose[60]; mouse mutants also show hyperglycemia and abnormal glucose homeostasis[61].

GLIS3 encodes the transcription factor GLIS family zinc finger 3 isoform, a Krüppel-like zinc finger protein that both activates and represses transcription and participates in beta-cell ontogeny[62,63]. Functional mutations in this gene cause a syndrome of neonatal diabetes and congenital hypothyroidism[63]. Polymorphisms within this gene have recently been associated with type 1 diabetes risk (t1dgc.org).

PROX1 encodes the prospero homeobox protein 1, a novel co-repressor of hepatocyte nuclear factor 4α[64] that plays a crucial role in beta-cell development; mutations in its target gene **HNF4A** cause maturity-onset diabetes of the young, type 1 (ref. 65).

C2CD4B (formerly **FAM148B**) encodes the nuclear localized factor 2 (NLF2). It is expressed in endothelial cells and upregulated by proinflammatory cytokines[66]. As shown here, it has a high level of expression in the pancreas, although its putative molecular connection with glucose homeostasis is presently unclear.

IGF1 encodes the insulin-like growth factor 1 and is the sole genome-wide significant locus associated with HOMA-IR in our study. Humans and mice null for IGF1 display abnormal glucose homeostasis, with insulin resistance, increased circulating insulin and insensitivity to growth hormone[67].

---

candidates; in *SLC2A2*, the lead SNP (rs11920090) is in perfect LD ($r^2 = 1.0$) with rs5400 (stage 1 discovery association $P = 5.9 \times 10^{-6}$), which codes for the amino acid substitution T110I, predicted to be "possibly damaging" by PolyPhen[35] and PANTHER (Pdel = 0.92)[36]. In *GCKR*, the lead SNP is in strong LD ($r^2 = 0.93$) with rs1260326, encoding P446L, a nonsynonymous variant previously associated with fasting glucose and HOMA-IR[11,12,30] and predicted by PolyPhen to be "probably damaging." A recent functional study has demonstrated that this variant indirectly leads to increased GCK activity, resulting in the observed effects on fasting glucose and triglyceride levels[37]. Both the *SLC2A2* T110I and *GCKR* P446L substitutions were predicted to be "tolerated" by SIFT[38], highlighting the difficulties in obtaining consensus functional predictions from different informatic approaches.

We used publicly available expression quantitative trait locus (eQTL) datasets for liver[39], cortex[40] and Epstein-Barr virus–transformed lymphoblastoid cell lines[41] to explore additional possible causal mechanisms by testing for association between replicated loci and mRNA expression levels of nearby genes (Online Methods). The lead SNP in *FADS1*, rs174550, is in strong LD with ($r^2 = 0.80$) and is in close proximity (130 bp) to rs174548, a SNP highly associated with *FADS1*

mRNA expression levels in liver ($P = 1.7 \times 10^{-5}$) and with *FADS2* mRNA expression levels in lymphoblastoid cells ($P = 3.1 \times 10^{-4}$). The SNP rs174548 has also been associated (up to $P = 4.5 \times 10^{-8}$) with a number of serum glycerophospholipid concentrations in a GWAS investigating metabolomic profiles[42], and rs174550 also showed strong associations ($P < 5.2 \times 10^{-7}$) with the same metabolites (data not shown). These results are substantiated by previous work associating SNPs in this region with the fatty acid composition of phospholipids[43]. The latter data suggest that the minor allele variant of rs174550 results in a reduced efficiency of the fatty acid delta-5 desaturase reaction[42]. Finally, bioinformatic analysis identifies a perfect proxy, rs174545 ($r^2 = 1.0$ with rs174550), whose glucose-raising allele abolishes a predicted target site for the miR-124 microRNA (see Online Methods). Taken together, these data support the hypothesis that not only the abundance of fatty acids, but also their precise composition and degree of desaturation, may influence glucose homeostasis.

Although our study was not designed to explicitly investigate the impact of copy number variation on glycemic traits, we took advantage of existing data[44] to investigate whether any of our lead SNPs are

in LD with common, diallelic copy number polymorphisms (CNPs) mapping within a 1-Mb window. Of the fasting glucose loci, only *DGKB-TMEM195* has a validated, common CNP affecting sequence within 1 Mb of the index SNP[44]. Despite the proximity of this CNP to the associated SNP (~25 kb), the CNP is essentially uncorrelated with the index SNP ($r^2 = 0.01$ in HapMap CEU) and is therefore unlikely to explain the observed association with fasting glucose level.

DISCUSSION

In this meta-analysis of 21 stage 1 discovery GWAS cohorts followed by targeted stage 2 replication of 25 loci in 33 additional cohorts (totaling up to 122,743 nondiabetic participants), we report new genome-wide significant associations of SNPs in or near *ADCY5*, *MADD*, *ADRA2A*, *CRY2*, *FADS1*, *GLIS3*, *SLC2A2*, *PROX1* and *C2CD4B* with fasting glucose and one SNP near *IGF1* associated with fasting insulin and HOMA-IR. We have also confirmed associations of variants in *GCK*, *GCKR*, *G6PC2* and *MTNR1B* with fasting glucose and achieved genome-wide significance for the recently reported *DGKB-TMEM195* locus[24] and for variants in the known T2D-associated genes *TCF7L2* and *SLC30A8*. All of the fasting glucose–associated SNPs showed consistent nominal associations with HOMA-B, and those in *GCK*, *G6PC2*, *MTNR1B*, *DGKB-TMEM195*, *ADCY5*, *FADS1* and *GLIS3* did so at genome-wide significant levels. As previously reported[11,12,30], *GCKR* is also associated with fasting insulin and HOMA-IR.

Notably, in addition to the established T2D-associated loci in *TCF7L2*, *SLC30A8* and *MTNR1B*, five of the loci that are associated with elevated fasting glucose levels in nondiabetic individuals (in *ADCY5*, *GCK*, *GCKR*, *PROX1* and *DGKB-TMEM195*) also increase the risk of T2D in separate T2D case-control studies. However, this overlap is incomplete and highlights the fact that the magnitude of the effect on fasting glucose is not predictive of the effect on T2D risk, as shown when comparing fasting glucose and T2D effect sizes for *MTNR1B* and *TCF7L2*, or for *ADCY5* and *MADD* (**Table 2**). Loci on the latter two genes have similar effect sizes on fasting glucose and have similar allele frequencies, and yet the former is robustly associated with T2D risk (OR 1.12, $P = 5.5 \times 10^{-21}$) whereas the latter is not (OR 1.01, $P = 0.3$) in the same samples. This suggests that not all loci associated with fasting glucose within the 'physiological' range are also associated with 'pathological' fasting glucose levels and T2D risk. Thus, variation in fasting glucose in healthy individuals is not necessarily an endophenotype for T2D, which posits the hypothesis that the mechanism by which glucose is raised, rather than a mere elevation in fasting glucose levels, is a key contributor to disease progression. On the other hand, we cannot rule out the existence of separate T2D-protective variants within loci for which elevated fasting glucose does not progress to manifest T2D; we also cannot rule out the effect of cohort selection in the detection of the loci with variable effects on fasting glucose and T2D risk. Nevertheless, this work shows that targeting quantitative traits in GWAS searches can help identify genetic determinants of overt disease.

With regard to insulin resistance, our analyses resulted in only one new genome-wide significant locus associated with fasting insulin and HOMA-IR. The associated SNP rs35767 is 1.2 kb upstream of *IGF1*, raising the possibility that it may influence *IGF1* expression levels (we have found no direct support for this notion in the limited eQTL data available). Although not reaching genome-wide significance, we note that SNP rs4675095 in *IRS1* (the insulin receptor substrate-1 gene) was also associated with HOMA-IR ($P = 4.6 \times 10^{-3}$), which, given *IRS1*'s excellent biological credentials, will warrant further investigation. This SNP is not in LD with the widely studied missense SNP substitution G972R (rs1801278), nor is it in LD with the newly discovered T2D SNP rs2943641 (ref. 45), whose C risk allele was only nominally

associated with increased fasting insulin ($P = 0.02$) and HOMA-IR ($P = 0.04$) in our discovery dataset. The previously reported associations of SNPs in *PANK1* with fasting insulin[24] did not receive strong support in our discovery cohorts ($P = 0.04$ and $P = 0.17$ for rs11185790 and rs1075374, respectively).

Notably, our large-scale meta-analyses produced more than a dozen robust associations with fasting glucose and only two with fasting insulin and HOMA-IR (*GCKR* and *IGF1*). Although the somewhat smaller sample size for the insulin analysis may have contributed to this discrepancy, a comparison of the similarly powered HOMA-B and HOMA-IR analyses reveals associations with HOMA-B several orders of magnitude more significant than those seen with HOMA-IR (**Fig. 2**). Because insulin itself is a component of the numerator in both measures, one cannot attribute this discrepancy to technical differences in insulin measurements across cohorts. Similarly, because the quantile-quantile plots are very similar for fasting insulin and HOMA-IR, we do not believe that the use of a mathematical formula (as was used with HOMA-IR) rather than a direct measurement (as was used with fasting insulin) has affected our analyses substantially. HOMA-B and HOMA-IR have comparable heritability estimates (0.26 and 0.27 in the Framingham Heart Study, respectively), and their correlation is substantial ($r = 0.55$ in the Framingham Heart Study). Thus, not only may there be a difference in the identity of specific genetic determinants for each trait[46], but the genetic architecture may be distinct for each trait, with more modest effects, fewer loci, rarer variants, or a stronger environmental modification underlying HOMA-IR. In addition, HOMA-IR (which is composed of fasting values) is an imperfect estimate of global insulin resistance, as it addresses mostly hepatic sensitivity to insulin and is partially affected by beta-cell function. The heritability of HOMA-IR is lower than the heritability for insulin sensitivity derived from the minimal model[47]. Exploration of gene × environment interactions and analysis of datasets that include 2-h glucose and insulin values may reveal other genetic factors that increase insulin resistance in humans[29].

In conclusion, our large-scale meta-analysis of GWAS has identified ten new loci associated with glycemic traits whose in-depth physiological investigation should further our understanding of glucose homeostasis in humans and may reveal new pathways for diabetes therapeutics.

METHODS

Methods and any associated references are available in the online version of the paper at http://www.nature.com/naturegenetics/.

Note: Supplementary information is available on the Nature Genetics website.

COMPETING INTERESTS STATEMENT
The authors declare competing financial interests: details accompany the full-text HTML version of the paper at http://www.nature.com/naturegenetics/.

Published online at http://www.nature.com/naturegenetics/.
Reprints and permissions information is available online at http://npg.nature.com/reprintsandpermissions/.

1. Genuth, S. *et al.* The Expert Committee on the Diagnosis and Classification of Diabetes Mellitus: Follow-up report on the diagnosis of diabetes mellitus. *Diabetes Care* **26**, 3160–3167 (2003).
2. Coutinho, M., Gerstein, H.C., Wang, Y. & Yusuf, S. The relationship between glucose and incident cardiovascular events. A metaregression analysis of published data from 20 studies of 95,783 individuals followed for 12.4 years. *Diabetes Care* **22**, 233–240 (1999).

3. Meigs, J.B., Nathan, D.M., D'Agostino, R.B. Sr. & Wilson, P.W. Fasting and postchallenge glycemia and cardiovascular disease risk: the Framingham Offspring Study. *Diabetes Care* **25**, 1845–1850 (2002).
4. UKPDS. Intensive blood-glucose control with sulphonylureas or insulin compared with conventional treatment and risk of complications in patients with type 2 diabetes (UKPDS 33). *Lancet* **352**, 837–853 (1998).
5. Patel, A. *et al.* Intensive blood glucose control and vascular outcomes in patients with type 2 diabetes. *N. Engl. J. Med.* **358**, 2560–2572 (2008).
6. Holman, R.R., Paul, S.K., Bethel, M.A., Matthews, D.R. & Neil, H.A. 10-year follow-up of intensive glucose control in type 2 diabetes. *N. Engl. J. Med.* **359**, 1577–1589 (2008).
7. Ray, K.K. *et al.* Effect of intensive control of glucose on cardiovascular outcomes and death in patients with diabetes mellitus: a meta-analysis of randomised controlled trials. *Lancet* **373**, 1765–1772 (2009).
8. Prokopenko, I., McCarthy, M.I. & Lindgren, C.M. Type 2 diabetes: new genes, new understanding. *Trends Genet.* **24**, 613–621 (2008).
9. Florez, J.C. Newly identified loci highlight beta cell dysfunction as a key cause of type 2 diabetes: Where are the insulin resistance genes? *Diabetologia* **51**, 1100–1110 (2008).
10. Weedon, M.N. *et al.* A common haplotype of the glucokinase gene alters fasting glucose and birth weight: association in six studies and population-genetics analyses. *Am. J. Hum. Genet.* **79**, 991–1001 (2006).
11. Sparsø, T. *et al.* The *GCKR* rs780094 polymorphism is associated with elevated fasting serum triacylglycerol, reduced fasting and OGTT-related insulinaemia, and reduced risk of type 2 diabetes. *Diabetologia* **51**, 70–75 (2008).
12. Orho-Melander, M. *et al.* A common missense variant in the glucokinase regulatory protein gene (*GCKR*) is associated with increased plasma triglyceride and C-reactive protein but lower fasting glucose concentrations. *Diabetes* **57**, 3112–3121 (2008).
13. Bouatia-Naji, N. *et al.* A polymorphism within the *G6PC2* gene is associated with fasting plasma glucose levels. *Science* **320**, 1085–1088 (2008).
14. Chen, W.-M. *et al.* Association studies in Caucasians identify variants in the *G6PC2/ABCB11* region regulating fasting glucose levels. *J. Clin. Invest.* **118**, 2620–2628 (2008).
15. Prokopenko, I. *et al.* Variants in *MTNR1B* influence fasting glucose levels. *Nat. Genet.* **41**, 77–81 (2009).
16. Lyssenko, V. *et al.* Common variant in *MTNR1B* associated with increased risk of type 2 diabetes and impaired early insulin secretion. *Nat. Genet.* **41**, 82–88 (2009).
17. Bouatia-Naji, N. *et al.* A variant near *MTNR1B* is associated with increased fasting plasma glucose levels and type 2 diabetes risk. *Nat. Genet.* **41**, 89–94 (2009).
18. Matthews, D.R. *et al.* Homeostasis model assessment: insulin resistance and β-cell function from fasting plasma glucose and insulin concentrations in man. *Diabetologia* **28**, 412–419 (1985).
19. Pe'er, I., Yelensky, R., Altshuler, D. & Daly, M.J. Estimation of the multiple testing burden for genomewide association studies of nearly all common variants. *Genet. Epidemiol.* **32**, 381–385 (2008).
20. Brunzell, J.D. *et al.* Relationships between fasting plasma glucose levels and insulin secretion during intravenous glucose tolerance tests. *J. Clin. Endocrinol. Metab.* **42**, 222–229 (1976).
21. Weir, G.C. & Bonner-Weir, S. Five stages of evolving β-cell dysfunction during progression to diabetes. *Diabetes* **53**, S16–S21 (2004).
22. Marchini, J., Howie, B., Myers, S., McVean, G. & Donnelly, P. A new multipoint method for genome-wide association studies by imputation of genotypes. *Nat. Genet.* **39**, 906–913 (2007).
23. Li, Y. & Mach Abecasis, G.R. 1.0: Rapid haplotype reconstruction and missing genotype inference. *Am. J. Hum. Genet.* **S79**, 2290 (2006).
24. Sabatti, C. *et al.* Genome-wide association analysis of metabolic traits in a birth cohort from a founder population. *Nat. Genet.* **41**, 35–46 (2009).
25. Diabetes Genetics Initiative of Broad Institute of Harvard and MIT, Lund University and Novartis Institutes for BioMedical Research. Genome-wide association analysis identifies loci for type 2 diabetes and triglyceride levels. *Science* **316**, 1331–1336 (2007).
26. Ioannidis, J.P., Ntzani, E.E., Trikalinos, T.A. & Contopoulos-Ioannidis, D.G. Replication validity of genetic association studies. *Nat. Genet.* **29**, 306–309 (2001).
27. Nejentsev, S., Walker, N., Riches, D., Egholm, M. & Todd, J.A. Rare variants of *IFIH1*, a gene implicated in antiviral responses, protect against type 1 diabetes. *Science* **324**, 387–389 (2009).
28. Tirosh, A. *et al.* Normal fasting plasma glucose levels and type 2 diabetes in young men. *N. Engl. J. Med.* **353**, 1454–1462 (2005).
29. Saxena, R. *et al.* Genetic variation in *GIPR* influences the glucose and insulin responses to an oral glucose challenge. *Nat. Genet.* advance online publication, doi:10.1038/ng.521 (17 January 2010).
30. Vaxillaire, M. *et al.* The common P446L polymorphism in *GCKR* inversely modulates fasting glucose and triglyceride levels and reduces type 2 diabetes risk in the DESIR prospective general French population. *Diabetes* **57**, 2253–2257 (2008).
31. Willer, C.J. *et al.* Six new loci associated with body mass index highlight a neuronal influence on body weight regulation. *Nat. Genet.* **41**, 25–34 (2009).
32. Newton-Cheh, C. *et al.* Eight blood pressure loci identified by genomewide association study of 34,433 people of European ancestry. *Nat. Genet.* **41**, 666–676 (2009).
33. Aulchenko, Y.S. *et al.* Loci influencing lipid levels and coronary heart disease risk in 16 European population cohorts. *Nat. Genet.* **41**, 47–55 (2009).
34. Kathiresan, S. *et al.* Common variants at 30 loci contribute to polygenic dyslipidemia. *Nat. Genet.* **41**, 56–65 (2009).
35. Sunyaev, S. *et al.* Prediction of deleterious human alleles. *Hum. Mol. Genet.* **10**, 591–597 (2001).
36. Thomas, P.D. *et al.* Applications for protein sequence-function evolution data: mRNA/protein expression analysis and coding SNP scoring tools. *Nucleic Acids Res.* **34**, W645–W650 (2006).
37. Beer, N.L. *et al.* The P446L variant in *GCKR* associated with fasting plasma glucose and triglyceride levels exerts its effect through increased glucokinase activity in liver. *Hum. Mol. Genet.* **18**, 4081–4088 (2009).
38. Ng, P.C. & Henikoff, S. Predicting deleterious amino acid substitutions. *Genome Res.* **11**, 863–874 (2001).
39. Schadt, E.E. *et al.* Mapping the genetic architecture of gene expression in human liver. *PLoS Biol.* **6**, e107 (2008).
40. Myers, A.J. *et al.* A survey of genetic human cortical gene expression. *Nat. Genet.* **39**, 1494–1499 (2007).
41. Dixon, A.L. *et al.* A genome-wide association study of global gene expression. *Nat. Genet.* **39**, 1202–1207 (2007).
42. Gieger, C. *et al.* Genetics meets metabolomics: a genome-wide association study of metabolite profiles in human serum. *PLoS Genet.* **4**, e1000282 (2008).
43. Schaeffer, L. *et al.* Common genetic variants of the *FADS1 FADS2* gene cluster and their reconstructed haplotypes are associated with the fatty acid composition in phospholipids. *Hum. Mol. Genet.* **15**, 1745–1756 (2006).
44. McCarroll, S.A. *et al.* Integrated detection and population-genetic analysis of SNPs and copy number variation. *Nat. Genet.* **40**, 1166–1174 (2008).
45. Rung, J. *et al.* Genetic variant near *IRS1* is associated with type 2 diabetes, insulin resistance and hyperinsulinemia. *Nat. Genet.* **41**, 1110–1115 (2009).
46. Doria, A., Patti, M.-E. & Kahn, C.R. The emerging genetic architecture of type 2 diabetes. *Cell Metab.* **8**, 186–200 (2008).
47. Bergman, R.N. *et al.* Minimal model-based insulin sensitivity has greater heritability and a different genetic basis than homeostasis model assessment or fasting insulin. *Diabetes* **52**, 2168–2174 (2003).
48. Higgins, J.P. & Thompson, S.G. Quantifying heterogeneity in a metaanalysis. *Stat. Med.* **21**, 1539–1558 (2002).
49. Peter-Riesch, B., Fathi, M., Schlegel, W. & Wollheim, C.B. Glucose and carbachol generate 1,2-diacylglycerols by different mechanisms in pancreatic islets. *J. Clin. Invest.* **81**, 1154–1161 (1988).
50. Prentki, M. & Matschinsky, F.M. Ca²⁺, cAMP, and phospholipid-derived messengers in coupling mechanisms of insulin secretion. *Physiol. Rev.* **67**, 1185–1248 (1987).
51. Drucker, D.J. The role of gut hormones in glucose homeostasis. *J. Clin. Invest.* **117**, 24–32 (2007).
52. Fukada, T. *et al.* The zinc transporter SLC39A13/ZIP13 is required for connective tissue development; its involvement in BMP/TGF-β signaling pathways. *PLoS One* **3**, e3642 (2008).
53. Mitro, N. *et al.* The nuclear receptor LXR is a glucose sensor. *Nature* **445**, 219–223 (2007).
54. Rorsman, P. *et al.* Activation by adrenaline of a low-conductance G protein-dependent K⁺ channel in mouse pancreatic β cells. *Nature* **349**, 77–79 (1991).
55. Keane, D. & Newsholme, P. Saturated and unsaturated (including arachidonic acid) non-esterified fatty acid modulation of insulin secretion from pancreatic β-cells. *Biochem. Soc. Trans.* **36**, 955–958 (2008).
56. Kume, K. *et al.* mCRY1 and mCRY2 are essential components of the negative limb of the circadian clock feedback loop. *Cell* **98**, 193–205 (1999).
57. Rudic, R.D. *et al.* BMAL1 and CLOCK, two essential components of the circadian clock, are involved in glucose homeostasis. *PLoS Biol.* **2**, e377 (2004).
58. Song, J.J. & Lee, Y.J. Cross-talk between JIP3 and JIP1 during glucose deprivation: SEK1–JNK2 and Akt1 act as mediators. *J. Biol. Chem.* **280**, 26845–26855 (2005).
59. Waeber, G. *et al.* The gene *MAPK8IP1*, encoding islet-brain-1, is a candidate for type 2 diabetes. *Nat. Genet.* **24**, 291–295 (2000).
60. Santer, R. *et al.* Mutations in *GLUT2*, the gene for the liver-type glucose transporter, in patients with Fanconi-Bickel syndrome. *Nat. Genet.* **17**, 324–326 (1997).
61. Guillam, M.T. *et al.* Early diabetes and abnormal postnatal pancreatic islet development in mice lacking Glut-2. *Nat. Genet.* **17**, 327–330 (1997).
62. Kim, Y.-S., Nakanishi, G., Lewandoski, M. & Jetten, A.M. GLIS3, a novel member of the GLIS subfamily of Kruppel-like zinc finger proteins with repressor and activation functions. *Nucleic Acids Res.* **31**, 5513–5525 (2003).
63. Senée, V. *et al.* Mutations in *GLIS3* are responsible for a rare syndrome with neonatal diabetes mellitus and congenital hypothyroidism. *Nat. Genet.* **38**, 682–687 (2006).
64. Song, K.-H., Li, T. & Chiang, J.Y.L. A prospero-related homeodomain protein is a novel co-regulator of hepatocyte nuclear factor 4α that regulates the cholesterol 7α-hydroxylase gene. *J. Biol. Chem.* **281**, 10081–10088 (2006).
65. Yamagata, K. *et al.* Mutations in the hepatocyte nuclear factor-4α gene in maturity-onset diabetes of the young (MODY1). *Nature* **384**, 458–460 (1996).
66. Warton, K., Foster, N.C., Gold, W.A. & Stanley, K.K. A novel gene family induced by acute inflammation in endothelial cells. *Gene* **342**, 85–95 (2004).
67. Clemmons, D.R. Role of insulin-like growth factor in maintaining normal glucose homeostasis. *Horm. Res.* **62** (Suppl. 1), 77–82 (2004).

Josée Dupuis[1,2,177], Claudia Langenberg[3,177], Inga Prokopenko[4,5,177], Richa Saxena[6,7,177], Nicole Soranzo[8,9,177], Anne U Jackson[10], Eleanor Wheeler[11], Nicole L Glazer[12], Nabila Bouatia-Naji[13], Anna L Gloyn[4], Cecilia M Lindgren[4,5], Reedik Mägi[4,5], Andrew P Morris[5], Joshua Randall[5], Toby Johnson[14–16], Paul Elliott[17,176], Denis Rybin[18], Gudmar Thorleifsson[19], Valgerdur Steinthorsdottir[19], Peter Henneman[20], Harald Grallert[21], Abbas Dehghan[22], Jouke Jan Hottenga[23], Christopher S Franklin[24], Pau Navarro[25], Kijoung Song[26], Anuj Goel[5,27], John R B Perry[28], Josephine M Egan[29], Taina Lajunen[30], Niels Grarup[31], Thomas Sparsø[31], Alex Doney[32], Benjamin F Voight[6,7], Heather M Stringham[10], Man Li[33], Stavroula Kanoni[34], Peter Shrader[35], Christine Cavalcanti-Proença[13], Meena Kumari[36], Lu Qi[37], Nicholas J Timpson[38], Christian Gieger[21], Carina Zabena[39], Ghislain Rocheleau[40,41], Erik Ingelsson[42,43], Ping An[44], Jeffrey O'Connell[45], Jian'an Luan[3], Amanda Elliott[6,7], Steven A McCarroll[6,7], Felicity Payne[11], Rosa Maria Roccasecca[11], François Pattou[46], Praveen Sethupathy[47], Kristin Ardlie[48], Yavuz Ariyurek[49], Beverley Balkau[50], Philip Barter[51], John P Beilby[52,53], Yoav Ben-Shlomo[54], Rafn Benediktsson[55,56], Amanda J Bennett[4], Sven Bergmann[14,16], Murielle Bochud[15], Eric Boerwinkle[57], Amélie Bonnefond[13], Lori L Bonnycastle[47], Knut Borch-Johnsen[58,59], Yvonne Böttcher[60], Eric Brunner[36], Suzannah J Bumpstead[8], Guillaume Charpentier[61], Yii-Der Ida Chen[62], Peter Chines[47], Robert Clarke[63], Lachlan J M Coin[17], Matthew N Cooper[64], Marilyn Cornelis[37], Gabe Crawford[6], Laura Crisponi[65], Ian N M Day[38], Eco J C de Geus[23], Jerome Delplanque[13], Christian Dina[13], Michael R Erdos[47], Annette C Fedson[64,66], Antje Fischer-Rosinsky[67,68], Nita G Forouhi[3], Caroline S Fox[2,69], Rune Frants[70], Maria Grazia Franzosi[71], Pilar Galan[72], Mark O Goodarzi[62], Jürgen Graessler[73], Christopher J Groves[4], Scott Grundy[74], Rhian Gwilliam[8], Ulf Gyllensten[75], Samy Hadjadj[76], Göran Hallmans[77], Naomi Hammond[8], Xijing Han[10], Anna-Liisa Hartikainen[78], Neelam Hassanali[4], Caroline Hayward[25], Simon C Heath[79], Serge Hercberg[80], Christian Herder[81], Andrew A Hicks[82], David R Hillman[66,83], Aroon D Hingorani[36], Albert Hofman[22], Jennie Hui[52,84], Joe Hung[85,86], Bo Isomaa[87,88], Paul R V Johnson[4,89], Torben Jørgensen[90,91], Antti Jula[92], Marika Kaakinen[93], Jaakko Kaprio[94–96], Y Antero Kesaniemi[97], Mika Kivimaki[36], Beatrice Knight[98], Seppo Koskinen[99], Peter Kovacs[100], Kirsten Ohm Kyvik[101], G Mark Lathrop[79], Debbie A Lawlor[38], Olivier Le Bacquer[13], Cécile Lecoeur[13], Yun Li[10], Valeriya Lyssenko[102], Robert Mahley[103], Massimo Mangino[9], Alisa K Manning[1], María Teresa Martínez-Larrad[39], Jarred B McAteer[6,104,105], Laura J McCulloch[4], Ruth McPherson[106], Christa Meisinger[21], David Melzer[28], David Meyre[13], Braxton D Mitchell[45], Mario A Morken[47], Sutapa Mukherjee[66,83], Silvia Naitza[65], Narisu Narisu[47], Matthew J Neville[4,107], Ben A Oostra[108], Marco Orrù[65], Ruth Pakyz[45], Colin N A Palmer[109], Giuseppe Paolisso[110], Cristian Pattaro[82], Daniel Pearson[47], John F Peden[5,27], Nancy L Pedersen[42], Markus Perola[96,111,112], Andreas F H Pfeiffer[67,68], Irene Pichler[82], Ozren Polasek[113], Danielle Posthuma[23,114], Simon C Potter[8], Anneli Pouta[115], Michael A Province[44], Bruce M Psaty[116,117], Wolfgang Rathmann[118], Nigel W Rayner[4,5], Kenneth Rice[119], Samuli Ripatti[96,111], Fernando Rivadeneira[22,120], Michael Roden[81,121], Olov Rolandsson[122], Annelli Sandbaek[123], Manjinder Sandhu[3,124], Serena Sanna[65], Avan Aihie Sayer[125], Paul Scheet[126], Laura J Scott[10], Udo Seedorf[127], Stephen J Sharp[3], Beverley Shields[98], Gunnar Sigurðsson[55,56], Eric J G Sijbrands[22,120], Angela Silveira[128], Laila Simpson[64,66], Andrew Singleton[129], Nicholas L Smith[130,131], Ulla Sovio[17], Amy Swift[47], Holly Syddall[125], Ann-Christine Syvänen[132], Toshiko Tanaka[133,134], Barbara Thorand[21], Jean Tichet[135], Anke Tönjes[60,136], Tiinamaija Tuomi[87,137], André G Uitterlinden[22,120], Ko Willems van Dijk[70,138], Mandy van Hoek[120], Dhiraj Varma[8], Sophie Visvikis-Siest[139], Veronique Vitart[25], Nicole Vogelzangs[140], Gérard Waeber[141], Peter J Wagner[96,111], Andrew Walley[142], G Bragi Walters[19], Kim L Ward[64,66], Hugh Watkins[5,27], Michael N Weedon[28], Sarah H Wild[24], Gonneke Willemsen[23], Jaqueline C M Witteman[22], John W G Yarnell[143], Eleftheria Zeggini[5,8], Diana Zelenika[79], Björn Zethelius[43,144], Guangju Zhai[9], Jing Hua Zhao[3], M Carola Zillikens[120], DIAGRAM Consortium[145], GIANT Consortium[145], Global BPgen Consortium[145], Ingrid B Borecki[44], Ruth J F Loos[3], Pierre Meneton[80], Patrik K E Magnusson[42], David M Nathan[104,105], Gordon H Williams[69,105], Andrew T Hattersley[98], Kaisa Silander[96,111], Veikko Salomaa[146], George Davey Smith[38], Stefan R Bornstein[73], Peter Schwarz[73], Joachim Spranger[67,68], Fredrik Karpe[4,107], Alan R Shuldiner[45], Cyrus Cooper[125], George V Dedoussis[34], Manuel Serrano-Ríos[39], Andrew D Morris[109], Lars Lind[132], Lyle J Palmer[64,66,84], Frank B Hu[147,148], Paul W Franks[149], Shah Ebrahim[150], Michael Marmot[36], W H Linda Kao[33,151,152], James S Pankow[153], Michael J Sampson[154], Johanna Kuusisto[155], Markku Laakso[155], Torben Hansen[31,156], Oluf Pedersen[31,59,157], Peter Paul Pramstaller[82,158,159], H Erich Wichmann[21,160,161], Thomas Illig[21], Igor Rudan[24,162,163], Alan F Wright[25], Michael Stumvoll[60], Harry Campbell[24], James F Wilson[24], Anders Hamsten on behalf of Procardis Consortium[128], Richard N Bergman[164], Thomas A Buchanan[164,165],

Francis S Collins[47], Karen L Mohlke[166], Jaakko Tuomilehto[94,167,168], Timo T Valle[167], David Altshuler[6,7,104,105], Jerome I Rotter[62], David S Siscovick[169], Brenda W J H Penninx[140], Dorret I Boomsma[23], Panos Deloukas[8], Timothy D Spector[8,9], Timothy M Frayling[28], Luigi Ferrucci[170], Augustine Kong[19], Unnur Thorsteinsdottir[19,171], Kari Stefansson[19,171], Cornelia M van Duijn[22], Yurii S Aulchenko[22], Antonio Cao[65], Angelo Scuteri[65,172], David Schlessinger[47], Manuela Uda[65], Aimo Ruokonen[173], Marjo-Riitta Jarvelin[17,93,174], Dawn M Waterworth[26], Peter Vollenweider[141], Leena Peltonen[8,48,96,111,112], Vincent Mooser[26], Goncalo R Abecasis[10], Nicholas J Wareham[3], Robert Sladek[40,41], Philippe Froguel[13,142], Richard M Watanabe[164,175], James B Meigs[35,105], Leif Groop[102], Michael Boehnke[10], Mark I McCarthy[4,5,107], Jose C Florez[6,7,104,105] & Inês Barroso[11] for the MAGIC investigators

[1]Department of Biostatistics, Boston University School of Public Health, Boston, Massachusetts, USA. [2]National Heart, Lung, and Blood Institute's Framingham Heart Study, Framingham, Massachusetts, USA. [3]Medical Research Council (MRC), Epidemiology Unit, Institute of Metabolic Science, Addenbrooke's Hospital, Cambridge, UK. [4]Oxford Centre for Diabetes, Endocrinology and Metabolism, University of Oxford, Oxford, UK. [5]Wellcome Trust Centre for Human Genetics, University of Oxford, Oxford, UK. [6]Program in Medical and Population Genetics, Broad Institute, Cambridge, Massachusetts, USA. [7]Center for Human Genetic Research, Massachusetts General Hospital, Boston, Massachusetts, USA. [8]Wellcome Trust Sanger Institute, Hinxton, Cambridge, UK. [9]Twin Research and Genetic Epidemiology Department, King's College London, St. Thomas' Hospital Campus, London, UK. [10]Center for Statistical Genetics, Department of Biostatistics, University of Michigan School of Public Health, Ann Arbor, Michigan, USA. [11]Metabolic Disease Group, Wellcome Trust Sanger Institute, Hinxton, Cambridge, UK. [12]Cardiovascular Health Research Unit and Department of Medicine, University of Washington, Seattle, Washington, USA. [13]Centre National de la Recherche Scientifique–Unité Mixte de Recherche 8090, Pasteur Institute, Lille 2–Droit et Santé University, Lille, France. [14]Department of Medical Genetics, University of Lausanne, Lausanne, Switzerland. [15]University Institute of Social and Preventative Medicine, Centre Hospitalier Universitaire Vaudois (CHUV) and University of Lausanne, Lausanne, Switzerland. [16]Swiss Institute of Bioinformatics, Lausanne, Switzerland. [17]Department of Epidemiology and Public Health, Imperial College London, Faculty of Medicine, Norfolk Place, London, UK. [18]Boston University Data Coordinating Center, Boston, Massachusetts, USA. [19]deCODE Genetics, Reykjavik, Iceland. [20]Department of Human Genetics, Leiden University Medical Centre, Leiden, The Netherlands. [21]Institute of Epidemiology, Helmholtz Zentrum Muenchen, German Research Center for Environmental Health, Neuherberg, Germany. [22]Department of Epidemiology, Erasmus Medical College, Rotterdam, The Netherlands. [23]Department of Biological Psychology, VU University Amsterdam, Amsterdam, The Netherlands. [24]Centre for Population Health Sciences, University of Edinburgh, Edinburgh, UK. [25]MRC Human Genetics Unit, Institute of Genetics and Molecular Medicine, Edinburgh, UK. [26]Division of Genetics, Research and Development, GlaxoSmithKline, King of Prussia, Pennsylvania, USA. [27]Department of Cardiovascular Medicine, University of Oxford, Oxford, UK. [28]Genetics of Complex Traits, Institute of Biomedical and Clinical Sciences, Peninsula College of Medicine and Dentistry, University of Exeter, Exeter, UK. [29]National Institute of Aging, Baltimore, Maryland, USA. [30]Unit for Child and Adolescent Health and Welfare, National Institute for Health and Welfare, Biocenter Oulu, University of Oulu, Oulu, Finland. [31]Hagedorn Research Institute, Gentofte, Denmark. [32]Department of Medicine and Therapeutics, Level 7, Ninewells Hospital and Medical School, Dundee, UK. [33]Department of Epidemiology, Bloomberg School of Public Health, Johns Hopkins University, Baltimore, Maryland, USA. [34]Department of Nutrition–Dietetics, Harokopio University, Athens, Greece. [35]General Medicine Division, Massachusetts General Hospital, Boston, Massachusetts, USA. [36]Department of Epidemiology and Public Health, University College London, London, UK. [37]Departments of Nutrition and Epidemiology, Harvard School of Public Health, Boston, Massachusetts, USA. [38]MRC Centre for Causal Analyses in Translational Epidemiology, University of Bristol, Bristol, UK. [39]Fundación para la Investigación Biomédica del Hospital Clínico San Carlos, Madrid, Spain. [40]Departments of Medicine and Human Genetics, McGill University, Montreal, Canada. [41]Genome Quebec Innovation Centre, Montreal, Canada. [42]Department of Medical Epidemiology and Biostatistics, Karolinska Institutet, Stockholm, Sweden. [43]Department of Public Health and Caring Sciences, Uppsala University, Uppsala, Sweden. [44]Division of Statistical Genomics, Department of Genetics, Washington University School of Medicine, St. Louis, Missouri, USA. [45]Division of Endocrinology, Diabetes and Nutrition, University of Maryland School of Medicine, Baltimore, Maryland, USA. [46]INSERM U859, Universite de Lille-Nord de France, Lille, France. [47]Genome Technology Branch, National Human Genome Research Institute, Bethesda, Maryland, USA. [48]The Broad Institute, Cambridge, Massachusetts, USA. [49]Leiden Genome Technology Center, Leiden University Medical Center, Leiden, The Netherlands. [50]INSERM U780, Paris Sud University, Villejuif, France. [51]The Heart Research Institute, Sydney, New South Wales, Australia. [52]PathWest Laboratory of Western Australia, Department of Molecular Genetics, J Block, QEII Medical Centre, Nedlands West Australia, Australia. [53]School of Surgery and Pathology, University of Western Australia, Nedlands West Australia, Australia. [54]Department of Social Medicine, University of Bristol, Bristol, UK. [55]Landspitali University Hospital, Reykjavik, Iceland. [56]Icelandic Heart Association, Kopavogur, Iceland. [57]The Human Genetics Center and Institute of Molecular Medicine, University of Texas Health Science Center, Houston, Texas, USA. [58]Steno Diabetes Center, Gentofte, Denmark. [59]Faculty of Health Science, University of Aarhus, Aarhus, Denmark. [60]Department of Medicine, University of Leipzig, Leipzig, Germany. [61]Endocrinology–Diabetology Unit, Corbeil-Essonnes Hospital, Essonnes, France. [62]Medical Genetics Institute, Cedars-Sinai Medical Center, Los Angeles, California, USA. [63]Clinical Trial Service Unit and Epidemiological Studies Unit, University of Oxford, Oxford, UK. [64]Centre for Genetic Epidemiology and Biostatistics, University of Western Australia, Perth, Australia. [65]Istituto di Neurogenetica e Neurofarmacologia (INN), Consiglio Nazionale delle Ricerche, c/o Cittadella Universitaria di Monserrato, Monserrato, Cagliari, Italy. [66]Western Australian Sleep Disorders Research Institute, Queen Elizabeth Medical Centre II, Perth, Australia. [67]Department of Endocrinology, Diabetes and Nutrition, Charite-Universitaetsmedizin Berlin, Berlin, Germany. [68]Department of Clinical Nutrition, German Institute of Human Nutrition Potsdam-Rehbruecke, Nuthetal, Germany. [69]Division of Endocrinology, Diabetes, and Hypertension, Brigham and Women's Hospital, Harvard Medical School, Boston, Massachusetts, USA. [70]Department of Human Genetics, Leiden University Medical Centre, Leiden, The Netherlands. [71]Department of Cardiovascular Research, Istituto di Ricerche Farmacologiche 'Mario Negri', Milan, Italy. [72]Institut National de la Santé et de la Recherche Médicale, Institut National de la Recherche Agronomique, Université Paris 13, Bobigny Cedex, France. [73]Department of Medicine III, Division Prevention and Care of Diabetes, University of Dresden, Dresden, Germany. [74]Center for Human Nutrition, University of Texas Southwestern Medical Center, Dallas, Texas, USA. [75]Department of Genetics and Pathology, Rudbeck Laboratory, Uppsala University, Uppsala, Sweden. [76]Centre Hospitalier Universitaire, de Poitiers, Endocrinologie Diabetologie, CIC INSERM 0802, INSERM U927, Université de Poitiers, Unité de Formation et de Recherche, Médecine Pharmacie, Poitiers, France. [77]Department of Public Health and Clinical Medicine, Section for Nutritional Research, Umeå University, Umeå, Sweden. [78]Department of Clinical Sciences, Obstetrics and Gynecology, University of Oulu, Oulu, Finland. [79]Centre National de Génotypage/Institut de génomique/Commissariat à l'énergie atomique, Evry Cedex, France. [80]INSERM U872, Faculté de Médecine Paris Descartes, Paris Cedex, France. [81]Institute for Clinical Diabetology, German Diabetes Center, Leibniz Center for Diabetes Research at Heinrich Heine University Düsseldorf, Düsseldorf, Germany. [82]Institute of Genetic Medicine, European Academy Bozen/Bolzano (EURAC), Viale Druso, Bolzano, Italy, Affiliated Institute of the University Lübeck, Lübeck, Germany. [83]Department of Pulmonary Physiology, Sir Charles Gairdner Hospital, Perth, Australia. [84]Busselton Population Medical Research Foundation, Sir Charles Gairdner Hospital, Perth, Australia. [85]Heart Institute of Western Australia, Sir Charles Gairdner Hospital, Nedlands West Australia, Australia. [86]School of Medicine and Pharmacology, University of Western Australia, Nedlands West Australia, Australia. [87]Folkhalsan Research Centre, Helsinki, Finland. [88]Malmska Municipal Health Care Center and Hospital, Jakobstad, Finland. [89]Nuffield Department of Surgery, University of Oxford, Oxford, UK. [90]Research Centre for Prevention and Health, Glostrup University Hospital, Glostrup, Denmark. [91]Faculty of Health Science, University of Copenhagen, Copenhagen, Denmark. [92]National Institute for Health and Welfare, Unit of Population Studies, Turku, Finland. [93]Institute of Health Sciences and Biocenter Oulu, University of Oulu, Oulu, Finland. [94]Department of Public Health, Faculty of Medicine, University of Helsinki, Helsinki, Finland. [95]National Institute for Health and Welfare, Unit for Child and Adolescent Mental Health, Helsinki, Finland. [96]Institute for Molecular Medicine Finland (FIMM), University of Helsinki, Helsinki, Finland. [97]Department of Internal Medicine and Biocenter Oulu, Oulu, Finland. [98]Diabetes Genetics, Institute of Biomedical and Clinical Science, Peninsula College of Medicine and Dentistry, University of Exeter, Exeter, UK. [99]National Institute for Health and Welfare, Unit of Living Conditions, Health and Wellbeing, Helsinki, Finland. [100]Interdisciplinary Centre for Clinical Research, University of Leipzig, Leipzig, Germany. [101]The Danish Twin

Registry, Epidemiology, Institute of Public Health, University of Southern Denmark, Odense, Denmark. [102]Department of Clinical Sciences, Diabetes and Endocrinology, Lund University, University Hospital Malmö, Malmö, Sweden. [103]Gladstone Institute of Cardiovascular Disease, University of California, San Francisco, California, USA. [104]Diabetes Research Center, Diabetes Unit, Massachusetts General Hospital, Boston, Massachusetts, USA. [105]Department of Medicine, Harvard Medical School, Boston, Massachusetts, USA. [106]Division of Cardiology, University of Ottawa Heart Institute, Ottawa, Ontario, Canada. [107]Oxford National Institute for Health Research, Biomedical Research Centre, Churchill Hospital, Oxford, UK. [108]Department of Clinical Genetics, Erasmus Medical College, Rotterdam, The Netherlands. [109]Biomedical Research Institute, University of Dundee, Ninewells Hospital and Medical School, Dundee, UK. [110]Department of Geriatric Medicine and Metabolic Disease, Second University of Naples, Naples, Italy. [111]National Institute for Health and Welfare, Unit of Public Health Genomics, Helsinki, Finland. [112]Department of Medical Genetics, University of Helsinki, Helsinki, Finland. [113]Department of Medical Statistics, Epidemiology and Medical Informatics, Andrija Stampar School of Public Health, Medical School, University of Zagreb, Rockefellerova, Zagreb, Croatia. [114]Department of Clinical Genetics, VU University and Medical Center, Amsterdam, The Netherlands. [115]Department of Obstetrics and Gynaecology, Oulu University Hospital, Oulu, Finland. [116]Departments of Medicine, Epidemiology and Health Services, University of Washington, Seattle, Washington, USA. [117]Group Health Research Institute, Group Health Cooperative, Seattle, Washington, USA. [118]Institute of Biometrics and Epidemiology, German Diabetes Centre, Leibniz Centre at Heinrich Heine University Düsseldorf, Düsseldorf, Germany. [119]Department of Biostatistics, University of Washington, Seattle, Washington, USA. [120]Department of Internal Medicine, Erasmus Medical College, Rotterdam, The Netherlands. [121]Department of Metabolic Diseases, Heinrich Heine University Düsseldorf, Düsseldorf, Germany. [122]Department of Public Health and Clinical Medicine, Section for Family Medicine, Umeå University, Umeå, Sweden. [123]School of Public Health, Department of General Practice, University of Aarhus, Aarhus, Denmark. [124]Department of Public Health and Primary Care, Strangeways Research Laboratory, University of Cambridge, Cambridge, UK. [125]MRC Epidemiology Resource Centre, University of Southampton, Southampton General Hospital, Southampton, UK. [126]Department of Epidemiology, University of Texas, M.D. Anderson Cancer Center, Houston, Texas, USA. [127]Leibniz-Institut für Arterioskleroseforschung an der Universität Münster, Münster, Germany. [128]Atherosclerosis Research Unit, Department of Medicine, Karolinska Institutet, Stockholm, Sweden. [129]Laboratory of Neurogenetics, National Institute on Aging, Bethesda, Maryland, USA. [130]Department of Epidemiology, University of Washington, Seattle, Washington, USA. [131]Seattle Epidemiologic Research and Information Center, Department of Veterans Affairs Office of Research and Development, Seattle, Washington, USA. [132]Department of Medical Sciences, Uppsala University, Uppsala, Sweden. [133]Medstar Research Institute, Baltimore, Maryland, USA. [134]Clinical Research Branch, National Institute on Aging, Baltimore, Maryland, USA. [135]Institut interrégional pour la santé (IRSA), La Riche, France. [136]Coordination Centre for Clinical Trials, University of Leipzig, Leipzig, Germany. [137]Department of Medicine, Helsinki University Hospital, University of Helsinki, Helsinki, Finland. [138]Department of Internal Medicine, Leiden University Medical Centre, Leiden, The Netherlands. [139]Research Unit, Cardiovascular Genetics, Nancy University Henri Poincaré, Nancy, France. [140]EMGO Institute for Health and Care Research, Department of Psychiatry, VU University Medical Center, Amsterdam, The Netherlands. [141]Department of Internal Medicine, Centre Hospitalier Universitaire Vaudois, Lausanne, Switzerland. [142]Genomic Medicine, Imperial College London, Hammersmith Hospital, London, UK. [143]Epidemiology and Public Health, Queen's University Belfast, Belfast, UK. [144]Medical Products Agency, Uppsala, Sweden. [145]See **Supplementary Note** for a full list of authors. [146]National Institute for Health and Welfare, Unit of Chronic Disease Epidemiology and Prevention, Helsinki, Finland. [147]Departments of Nutrition and Epidemiology, Harvard School of Public Health, Boston, Massachusetts, USA. [148]Channing Laboratory, Brigham and Women's Hospital and Harvard Medical School, Boston, Massachusetts, USA. [149]Genetic Epidemiology and Clinical Research Group, Department of Public Health and Clinical Medicine, Section for Medicine, Umeå University Hospital, Umeå, Sweden. [150]London School of Hygiene and Tropical Medicine, London, UK. [151]Department of Medicine, School of Medicine, Johns Hopkins University, Baltimore, Maryland, USA. [152]The Welch Center for Prevention, Epidemiology, and Clinical Research, School of Medicine and Bloomberg School of Public Health, Johns Hopkins University, Baltimore, Maryland, USA. [153]Division of Epidemiology and Community Health, School of Public Health, University of Minnesota, Minneapolis, Minnesota, USA. [154]Department of Endocrinology and Diabetes, Norfolk and Norwich University Hospital National Health Service Trust, Norwich, UK. [155]Department of Medicine, University of Kuopio and Kuopio University Hospital, Kuopio, Finland. [156]Faculty of Health Science, University of Southern Denmark, Odense, Denmark. [157]Institute of Biomedical Science, Faculty of Health Science, University of Copenhagen, Copenhagen, Denmark. [158]Department of Neurology, General Central Hospital, Bolzano, Italy. [159]Department of Neurology, University of Lübeck, Lübeck, Germany. [160]Institute of Medical Informatics, Biometry and Epidemiology, Ludwig-Maximilians-Universität, Munich, Germany. [161]Klinikum Grosshadern, Munich, Germany. [162]School of Medicine, University of Split, Split, Croatia. [163]Gen-Info Ltd., Zagreb, Croatia. [164]Department of Physiology and Biophysics, Keck School of Medicine, University of Southern California, Los Angeles, California, USA. [165]Department of Medicine, Division of Endocrinology, Keck School of Medicine, University of Southern California, Los Angeles, California, USA. [166]Department of Genetics, University of North Carolina, Chapel Hill, North Carolina, USA. [167]National Institute for Health and Welfare, Unit of Diabetes Prevention, Helsinki, Finland. [168]South Ostrobothnia Central Hospital, Seinajoki, Finland. [169]Departments of Medicine and Epidemiology, University of Washington, Seattle, Washington, USA. [170]Longitudinal Studies Section, Clinical Research Branch, National Institute on Aging, NIH, Baltimore, Maryland, USA. [171]Faculty of Medicine, University of Iceland, Reykjavík, Iceland. [172]Lab of Cardiovascular Sciences, National Institute on Aging, National Institutes of Health, Baltimore, Maryland, USA. [173]Department of Clinical Sciences/Clinical Chemistry, University of Oulu, Oulu, Finland. [174]National Institute of Health and Welfare, Oulu, Finland. [175]Department of Preventive Medicine, Keck School of Medicine, University of Southern California, Los Angeles, California, USA. [176]MRC–Health Protection Agency Centre for Environment and Health, Imperial College London, London, UK. [177]These authors contributed equally to this work. Correspondence should be addressed to M.B. (boehnke@umich.edu), M.I.M. (mark.mccarthy@drl.ox.ac.uk), J.C.F. (jcflorez@partners.org) or I.B. (ib1@sanger.ac.uk).

ONLINE METHODS

Cohort description. The consortia participating in MAGIC contributed a maximum total of 122,743 individuals. The stage 1 discovery set included 36,466–46,186 individuals (depending on trait) from 17 population-based cohort studies and four case-control studies. The stage 2 replication set included up to 76,558 individuals from 33 sample collections, including 28 population-based and 5 case-control collections. Detailed information on all studies is provided in **Supplementary Table 1a** (stage 1 discovery) and **1b** (stage 2 replication). All participants were adults of white European ancestry from the United States or Europe. Individuals were excluded from the analysis if they had a physician diagnosis of diabetes, were on diabetes treatment (oral or insulin) or had a fasting plasma glucose ≥7 mmol/l. Some individuals with fasting glucose <7 mmol/l but who would have tested abnormally after an oral glucose challenge could have been included; we estimated this number to be as low as <1% in the Framingham Heart Study and 1.6% in Inter99, two population cohorts in which all relevant data were available. Individual studies applied further sample exclusions, including pregnancy, non-fasting individuals, type 1 diabetes, or outliers ±3 s.d. of distribution for either fasting glucose or fasting insulin, as detailed in **Supplementary Table 1a** and **1b**. Individual stage 1 discovery cohort sizes ranged between 458 and 6,479 samples; stage 2 replication cohorts ranged between 554 and 8,010 samples. All studies were approved by local research ethic committees, and all participants gave informed consent.

Type 2 diabetes association. The association analysis of lead SNPs with T2D as a dichotomous trait was carried out under the additive genetic model in 27 case-control cohorts totaling 40,655 cases and 87,022 controls of European descent. These included 8,130 cases and 38,987 controls from eight DIAGRAM+ Consortium studies and 32,525 additional T2D cases and 48,035 additional controls from 19 cohorts genotyped *de novo*, listed as cohort (*n* cases/*n* controls): FUSION_stage2 (1,203/1,261), METSIM_CC (854/3,469), Addition/Ely (892/1,612), Cambridgeshire Case Control Study (541/527), Norfolk Diabetes Case Control Study (6,056/6,428), deCODE (1,465/23,194), DGDG (690/730), DGI (1,022/1,075), ERGO (1,178/4,761), EUROSPAN (268/3,710), FUSION (1,161/1,174), KORA S3 (433/1,438), T2D Wellcome Trust Case Control Consortium (1,924/2,938), HPFS (1,146/1,241), Nurses' Health Study (1,532/1,754), Danish (3,652/4,992), KORA_replication consisting of cases from KORAS1-S4 and the Augsburg Diabetes Family Study (ADFS) and controls from KORA S4 (1,047/1,491), OxGN_58BC (UKRS2) (612/1,596), UKT2DGC (4,979/6,454), Framingham Heart Study_CC (674/7,664), NHANES (289/1,219), Partners/Roche (534/649), Umeå (1,327/1,424), French_CC (2,155/1,862), GCI Poland_DGI_Stage2 (969/969), GCI_US_DGI_Stage2 (1,191/1,171) and MDC_MDR_DGI_Stage2 (2,814/3,234). According to the best sample-specific model, in some cohorts, age and BMI were used as covariates for adjustment of the case-control association. The meta-analysis of the cohort-specific summary statistics (odds ratios and 95% confidence intervals) was performed using a fixed effects inverse-variance approach with GWAMA (see URLs).

Quantitative trait measurements. Fasting glucose (in mmol/l) was measured from fasting whole blood, plasma or serum or a combination of these. Whole-blood fasting glucose levels were corrected to plasma fasting glucose using a correction factor of 1.13. Fasting insulin was measured as described in **Supplementary Table 1a** and **1b** for each of the cohorts. Indices of beta-cell function (HOMA-B) and insulin resistance (HOMA-IR) were derived from paired fasting glucose and insulin measures using the homeostasis model assessment[18].

Genotyping, imputation and quality control. Genotyping of individual cohorts was carried out using commercial genome-wide arrays as detailed in **Supplementary Table 1a** and **1b**. For genome-wide SNP sets, different criteria were used to filter out poor-quality SNPs and samples before imputation. Criteria generally applied for exclusion of samples were (i) call-rate <0.95, (ii) individuals with heterozygosity outside the population-specific bounds and (iii) ethnic outliers. Criteria generally applied for exclusion of SNPs were (i) minor allele frequency (MAF) <0.01, (ii) Hardy-Weinberg equilibrium $P < 10^{-4}$ or 10^{-6} and (iii) call-rate <0.95. Imputation of additional autosomal SNPs from the HapMap CEU reference panel was performed using the software MACH[23], IMPUTE[22] or BIMBAM[68] with parameters and pre-imputation filters as specified in **Supplementary Table 1a** and **1b**. SNPs were also excluded if the cohort-specific imputation quality as assessed by r2.hat was <0.3 (MACH) or proper-info was <0.4 (IMPUTE) or observed/expected dosage variance was <0.3 (BIMBAM), or if their mapping and/or strand annotation was ambiguous. In total, up to 2.5 million genotyped or imputed autosomal SNPs were considered for meta-analysis. SNPs were considered for meta-analysis if they were available for at least 20% of maximum available sample size or if ≥10,000 individuals were informative for each SNP.

Statistical analyses. We excluded from analysis people with diabetes (those on diabetes treatment or with fasting glucose ≥7 mmol/l), non-fasting participants and pregnant women. In each cohort, we used log-transformed trait values for fasting insulin, HOMA-IR and HOMA-B and untransformed fasting glucose as the dependent variable in linear regression models that included terms for sex, age (except NFBC 1966, where all subjects were 31 years old), study site (if applicable), geographical covariates (if applicable) and age squared (Framingham only) to assess the association of additively coded genotypes with trait values. Association testing was performed using software that takes genotype and imputation uncertainty into account, using a missing-data likelihood test implemented in SNPTEST[22] or by using allele dosages in the linear regression model in MACH2QTL[23], GenABEL[69] or lmekin from the R kinship package[70]. Regression estimates for the effect of the additively coded SNP were pooled across studies in a meta-analysis using a fixed effect inverse-variance approach[71]. The individual cohort results, but not the final meta-analysis results, were corrected for residual inflation of the test statistic using the genomic control method[72]. Final GC values were 1.05 for fasting glucose, 1.046 for HOMA-B, 1.04 for HOMA-IR and 1.041 for fasting insulin.

Replication SNP selection and analysis. Twenty-five lead SNPs from among the most significant association results in the stage 1 discovery meta-analyses were selected for replication. To account for the correlation between traits and to ensure independent signals, highly significant associations detected in two or more traits were selected only once. All selected loci had an $r^2 < 0.5$ with the nearest other selected loci. From each unique locus, the SNP with the smallest P value was chosen. All SNPs had a minimum sample size of at least 80% of the overall discovery sample. Variants known to be associated with T2D (in *SLC30A8* and *TCF7L2*) and reaching the genome-wide significance threshold ($P < 5 \times 10^{-8}$) were not included in the replication list. SNPs were also selected on the basis of low heterogeneity between studies, although loci with biologic plausibility were selected even if there was some evidence of heterogeneity. Seventeen SNPs from the glucose and HOMA-B analyses and eight SNPs from the insulin and HOMA-IR analyses were selected for stage 2 replication. Although previously described, variants in *G6PC2*, *GCK*, *GCKR* and *MTNR1B* were selected for replication to serve as 'positive controls' in all study samples. Up to four alternate proxy SNPs (maximizing LD with the index SNP) were selected for each locus to accommodate the capacities of different platforms. In the cases where index SNPs failed in the initial stage of genotyping, replication results were obtained for proxy SNPs in strong LD with the original index SNP whenever possible. SNPs with Hardy-Weinberg equilibrium P values ≤0.001 were excluded. In cases where more than one proxy SNP was genotyped but the index SNP was unavailable, the proxy SNP's LD with the index SNP and its call rate was used to select the SNP with the best-quality genotyping to be included in the meta-analysis.

Genotype data for 25 signals or proxies were obtained from 33 independent replication cohorts, including both *in silico* data from pre-existing GWAS (8) and *de novo* genotyping (25). Phenotype definition and association testing between fasting traits and these 25 SNPs was performed in the same manner in each cohort. The inverse variance method was then applied to derive pooled effect estimates from the stage 2 replication samples using METAL (see URLs) and GWAMA software. We then carried out a pooled analysis of the stage 1 discovery cohorts and stage 2 replication samples to determine which SNPs reached genome-wide significance, as determined by a $P < 5 \times 10^{-8}$. Heterogeneity was assessed using the I^2 index[48].

Notes on replication genotyping. *Amish.* The Amish trait data is reported for the Heredity and Phenotype Interaction Heart Study (HAPI), Amish Family Longevity Study (LS), Amish Family Diabetes Study (AFDS), Amish

Family Calcification Study (AFCS) and Pharmacogenomics of Anti-Platelet Intervention (PAPI) Study. All studies genotyped 15 SNPs (rs10830963, rs4607517, rs11605924, rs11708067, rs1416802, rs588262, rs4675095, rs6947696, rs4912494, rs11920090, rs174550, rs7034200, rs4243291, rs457420, rs1881413). Other SNPs were typed on different sample subsets: AFDS only (rs2191349, rs10493846); HAPI only (rs560887); HAPI, LS and Pharmacogenomics of Anti-Platelet Interaction study (PAPI) (rs780094, rs6479526, rs340835, rs11167682); HAPI, LS, AFDS, PAPI (rs4918635, rs855228); HAPI, LS and AFCS (rs11039149). The genotyping statistics in **Supplementary Table 1b** are reported for the AFDS + HAPI + LS cohorts.

FUSION stage 2. The FUSION stage 2 cohort includes some Health 2000 samples, none of which overlap with the Health 2000 cohort.

SNP score. For the 16 SNPs reaching genome-wide significance of association (either in the discovery stage alone or in the combined replication and discovery meta-analysis), we defined a risk score as the weighted sum of the number of expected risk alleles, where the sum of the weights was set to the number of SNPs (16) and the weights were proportional to the estimate of the effect size for each SNP. Mean fasting glucose levels according to the number of weighted risk alleles were computed in some of the largest cohorts (Framingham, ARIC, NFBC 1966) with all 16 SNPs available (genotyped or imputed).

Bioinformatic analysis and functional annotation. To perform a preliminary assessment of the underlying functionality at the associated loci, we first expanded the set of SNPs to include those in strong LD with the index SNP (defined as pairwise $r^2 > 0.8$ according to HapMap Phase II CEU data). We then mapped the genomic locations of all the SNPs in this expanded set to several non-mutually-exclusive genomic annotation sets: nonsynonymous sites, splice sites, intergenic regions, 5′ UTR, 3′ UTR and introns from dbSNP version 129 (see URLs section for URLs of this and other software mentioned in this paragraph); 1-kb and 5-kb regions upstream of transcription start sites from Ensembl version 49; intergenic predicted transcription factor binding sites, CpG islands, ORegAnno elements, Encode region ancestral repeats, EvoFold elements, multispecies conserved sequences and positively selected gene regions from the University of California Santa Cruz human table browser; predicted microRNA target sites from TargetScan 4.2; validated enhancers from the Vista Enhancer Browser; predicted *cis*-regulatory modules from the PreMod database; and validated noncoding RNAs from RNAdb. The potential functional effect of nonsynonymous substitutions were evaluated using three prediction programs: SIFT, PolyPhen and PANTHER.

GRAIL. We used GRAIL (see URLs) to examine the putative relationship between candidate genes at validated loci based on concomitant appearance in published scientific text. GRAIL is a bioinformatic annotation tool that, given several genomic regions or SNPs associated with a particular phenotype or disease, searches for similarities in the published scientific text among the associated genes[73]. It scores regions for functional relatedness by defining associated regions based on the interval between recombination hotspots flanking furthest neighboring SNPs with $r^2 > 0.5$ to the index SNP, and identifies overlapping genes in that region. Based on textual relationships between genes (as determined from a download of PubMed abstracts on 16 December 2006), GRAIL assigns a *P* value to each region suggesting its degree of functional connectivity, and picks the best candidate gene after taking into account multiple comparisons.

We considered the following SNPs and candidate genes: rs10830963 (*MTNR1B*), rs2191349 (*DGKB*), rs4607517 (*GCK*), rs11920090 (*SLC2A2*), rs11708067 (*ADCY5*), rs560887 (*G6PC2*), rs780094 (*GCKR*), rs11605924 (*CRY2*), rs7034200 (*GLIS3*), rs340874 (*PROX1*), rs10885122 (*ADRA2A*), rs7944584 (*NR1H3*), rs174550 (*FEN1, FADS1, C11orf9, C11orf10, FADS2*) and rs11071657 (*C2CD4B*). In addition, the following keywords describing functional connections were used: "glucose", "diabetes", "islet", "diacylglycerol", "circadian", "insulin", "drosophila", "liver", "clock", "cyclase", "pancreatic", "adenylyl", "memory", "beta", "mice", "islets", "phosphatase", "camp", "light", "activity". A total of 7 genes (*MTNR1B, DGKB, GCK, SLC2A2, ADCY5, G6PC2* and *GCKR*) out of 14 had a significant association with functional connectivity (at $P < 0.1$) compared to 1.4 expected under the null, demonstrating that this gene set is enriched in relationships with each other.

eQTL analysis. The validated association signals were searched for previous evidence of expression quantitative trait loci (eQTLs) using several data sources. Liver eQTL association results were obtained from Schadt *et al.*[39]. Cortex eQTL association results were obtained from Myers *et al.*[40]. Epstein-Barr virus-transformed lymphoblastoid cell eQTLs from ref. 41 were retrieved using the mRNA by SNP browser (see URLs). For each region, we limited our analysis to *cis* eQTLs given the difficulty of reliably interpreting *trans* effects. Genes or SNPs within 1 Mb from the lead SNP were considered. The r^2 values between the lead SNPs and eQTL SNPs were retrieved from the HapMap Phase 2 data (CEU Panel), and only SNPs with $r^2 > 0.6$ were considered.

Of the 12 SNPs showing association with liver and located at < 1 Mb from the lead SNP, five had no r^2 data in HapMap and were located at large distances from the MAGIC lead SNP (mean 320 kb, range 48-725 kb). Of the remaining seven, rs174548 at the *FADS1* (fatty acid desaturase 1, $P_{eQTL} = 1.74 \times 10^{-5}$) locus was located 130 bp away from the lead SNP rs174550 and in strong LD (pairwise $r^2 = 0.8$). All the remaining SNPs did not fit our criteria for selection, although we note that a second lead SNP (rs780094 at *GCKR*) was also moderately associated ($r^2 = 0.49$, distance = 74 kb) with a strong effect eQTL (rs4665969 at *IFT172*, $P_{eQTL} = 3.97 \times 10^{-23}$). For circulating lymphoblastoid cells, the only *cis* effect fitting our criteria was observed for the MAGIC SNP rs174550 (*FADS1*), which was located 24 kb from a known eQTL centered on the *FADS2* gene ($P_{eQTL} = 3.1 \times 10^{-4}$). Finally, for cortex, the only eQTL was found at four SNPs within *LOC131076* (rs6769837, rs7648255, rs12636058, rs6438726), all located >870 kb from the MAGIC lead SNP (rs11708067 at *ADCY5*, LD metrics not available).

Gene expression studies. Adult total RNA samples, except pancreatic islets and flow-sorted beta cells, were purchased from Clontech (Clontech-Takara Bio Europe, Saint-Germain-en-Laye, France). Adult human islets ($n = 2$) were available through existing collections at Oxford University and were obtained with full ethical consent. Flow-sorted beta cells were obtained from two brain-dead adult donors (preparations >92% insulin-positive cells), in accordance with French legislation and the local ethical committee, as previously described[74].

Tissue panel (Oxford). Samples were treated with DNase I (Ambion) to ensure that residual genomic contamination was removed. For each tissue, 1 μg of total RNA was used to generate cDNA by random primed first strand synthesis (Applied Biosystems) according to the manufacturer's protocol. Reverse transcription was also performed on all samples in the absence of the enzyme reverse transcriptase, and these samples were used as negative controls. Primers were designed to cover all RefSeq transcripts. Resulting cDNA for each tissue was diluted 1:100 and 4 μl used in a 10 μl qRT-PCR reaction with 5.5 μl gene expression master mix (Applied Biosystems) and 0.5 μl gene specific assay (Applied Biosystems). All samples were run in triplicate. A standard curve was generated by pooling 1 μl of each cDNA and serially diluting (1:50, 1:100, 1:200, 1:400, 1:800) and running as above. Expression levels were determined with respect to the mean of four endogenous controls (β-actin, B2M, HPRT, TOP1) and normalizing to the mean of the 1:100 standard for the assay of interest. For ease of presentation, the maximum gene expression has been set to equal 1 and all other tissue expressions reported as a fraction of this.

Tissue panel (Cambridge). Adult human total RNA samples (cerebellum, cortex, spleen, pancreas, lung, kidney, liver, skeletal muscle, heart, testes, adipocyte and total brain) were obtained from Clontech. Random-primed first-strand cDNA synthesis was performed with 100 ng RNA using Super Script II (Invitrogen) according to manufacturer's instructions. Primers were design to cover the majority of protein coding transcripts. For the standard curve, 200 ng of a pool of all RNA samples was amplified using the same protocol. The resulting cDNA for each tissue was diluted fivefold and 5 μl of each sample were used in a 12 μl SYBR Green PCR Master Mix (Applied Biosystem). The cDNA for the standard curve was diluted twofold and used as above. Primers (SIGMA) were designed to anneal to all annotated isoforms of any given gene. Quantitative PCR reactions were done in triplicate on an ABI 7900HT (Applied Biosystems). Expression levels were calculated from their average crossing points, expressed relative to the control gene *Top1* (encoding topoisomerase 1), and normalized to gene-specific expression in pancreas. For the purpose of presentation, for each gene the maximal expression was set to equal one and the rest reported as fraction of this

number. The results of these duplicate experiments, which largely confirm those reported in the text, are shown in **Supplementary Figure 3**.

Flow-sorted beta cells (Lille). Samples were treated with DNase I (Ambion) to ensure that residual genomic contamination was removed. For each tissue, 1 µg of total RNA was used to generate cDNA by random primed first strand synthesis (Applied Biosystems) according to the manufacturer's protocol. Reverse transcription was also performed on all samples in the absence of the enzyme reverse transcriptase, and these samples were used as negative controls. Total RNA was extracted using Nucleospin RNA II kit (Macherey Nagel) according to the manufacturer's instructions. Resulting cDNA for each tissue was diluted 1:10, and 4 µl was used in a 20-µl qRT-PCR reaction with 10 µl gene expression master mix (Applied Biosystems) and 1 µl gene-specific assay (Applied Biosystems). Data is presented with the most expressed gene (*GLIS3*) normalized to 1 and all other genes reported as a fraction of this number.

URLs. GWAMA, http://www.well.ox.ac.uk/gwama/index.shtml; METAL, http://www.sph.umich.edu/csg/abecasis/Metal/index.html; dbSNP version 129, http://www.ncbi.nlm.nih.gov/projects/SNP/; Ensembl version 49, http://www.ensembl.org; University of California Santa Cruz human table browser, http://genome.ucsc.edu/cgi-bin/hgTables; TargetScan 4.2, http://www.targetscan.org; Vista Enhancer Browser, http://enhancer.lbl.gov; PreMod database, http://genomequebec.mcgill.ca/PreMod; RNAdb, http://research. imb.uq.edu.au/rnadb/; SIFT, http://blocks.fhcrc.org/sift/SIFT.html; PolyPhen, http://genetics.bwh.harvard.edu/pph/; PANTHER, http://www.pantherdb.org/tools/csnpScoreForm.jsp; GRAIL (Gene Relationships Across Implicated Loci), http://www.broad.mit.edu/mpg/grail; mRNA by SNP browser, http://www.sph.umich.edu/csg/liang/asthma/.

68. Servin, B. & Stephens, M. Imputation-based analysis of association studies: candidate regions and quantitative traits. *PLoS Genet.* **3**, e114 (2007).
69. Aulchenko, Y.S., Ripke, S., Isaacs, A. & van Duijn, C.M. GenABEL: an R library for genome-wide association analysis. *Bioinformatics* **23**, 1294–1296 (2007).
70. R Development Core Team. *R: A Language and Environment for Statistical Computing* (R Foundation for Statistical Computing, Vienna, 2007).
71. Petitti, D.B. Statistical methods in meta-analysis. in *Meta-analysis, Decision Analysis, and Cost-effectiveness Analysis* (ed. Petitti, D.B.) 94–118 (Oxford University Press, New York, 2000).
72. Devlin, B. & Roeder, K. Genomic control for association studies. *Biometrics* **55**, 997–1004 (1999).
73. Raychaudhuri, S. *et al.* Identifying relationships among genomic disease regions: predicting genes at pathogenic SNP associations and rare deletions. *PLoS Genet.* **5**, e1000534 (2009).
74. Lukowiak, B. *et al.* Identification and purification of functional human β-cells by a new specific zinc-fluorescent probe. *J. Histochem. Cytochem.* **49**, 519–528 (2001).

Erratum: New genetic loci implicated in fasting glucose homeostasis and their impact on type 2 diabetes risk

Josée Dupuis, Claudia Langenberg, Inga Prokopenko, Richa Saxena, Nicole Soranzo, Anne U Jackson, Eleanor Wheeler, Nicole L Glazer, Nabila Bouatia-Naji, Anna L Gloyn, Cecilia M Lindgren, Reedik Mägi, Andrew P Morris, Joshua Randall, Toby Johnson, Paul Elliott, Denis Rybin, Gudmar Thorleifsson, Valgerdur Steinthorsdottir, Peter Henneman, Harald Grallert, Abbas Dehghan, Jouke Jan Hottenga, Christopher S Franklin, Pau Navarro, Kijoung Song, Anuj Goel, John R B Perry, Josephine M Egan, Taina Lajunen, Niels Grarup, Thomas Sparsø, Alex Doney, Benjamin F Voight, Heather M Stringham, Man Li, Stavroula Kanoni, Peter Shrader, Christine Cavalcanti-Proença, Meena Kumari, Lu Qi, Nicholas J Timpson, Christian Gieger, Carina Zabena, Ghislain Rocheleau, Erik Ingelsson, Ping An, Jeffrey O'Connell, Jian'an Luan, Amanda Elliott, Steven A McCarroll, Felicity Payne, Rosa Maria Roccasecca, François Pattou, Praveen Sethupathy, Kristin Ardlie, Yavuz Ariyurek, Beverley Balkau, Philip Barter, John P Beilby, Yoav Ben-Shlomo, Rafn Benediktsson, Amanda J Bennett, Sven Bergmann, Murielle Bochud, Eric Boerwinkle, Amélie Bonnefond, Lori L Bonnycastle, Knut Borch-Johnsen, Yvonne Böttcher, Eric Brunner, Suzannah J Bumpstead, Guillaume Charpentier, Yii-Der Ida Chen, Peter Chines, Robert Clarke, Lachlan J M Coin, Matthew N Cooper, Marilyn Cornelis, Gabe Crawford, Laura Crisponi, Ian N M Day, Eco J C de Geus, Jerome Delplanque, Christian Dina, Michael R Erdos, Annette C Fedson, Antje Fischer-Rosinsky, Nita G Forouhi, Caroline S Fox, Rune Frants, Maria Grazia Franzosi, Pilar Galan, Mark O Goodarzi, Jürgen Graessler, Christopher J Groves, Scott Grundy, Rhian Gwilliam, Ulf Gyllensten, Samy Hadjadj, Göran Hallmans, Naomi Hammond, Xijing Han, Anna-Liisa Hartikainen, Neelam Hassanali, Caroline Hayward, Simon C Heath, Serge Hercberg, Christian Herder, Andrew A Hicks, David R Hillman, Aroon D Hingorani, Albert Hofman, Jennie Hui, Joe Hung, Bo Isomaa, Paul R V Johnson, Torben Jørgensen, Antti Jula, Marika Kaakinen, Jaakko Kaprio, Y Antero Kesaniemi, Mika Kivimaki, Beatrice Knight, Seppo Koskinen, Peter Kovacs, Kirsten Ohm Kyvik, G Mark Lathrop, Debbie A Lawlor, Olivier Le Bacquer, Cécile Lecoeur, Yun Li, Valeriya Lyssenko, Robert Mahley, Massimo Mangino, Alisa K Manning, María Teresa Martínez-Larrad, Jarred B McAteer, Laura J McCulloch, Ruth McPherson, Christa Meisinger, David Melzer, David Meyre, Braxton D Mitchell, Mario A Morken, Sutapa Mukherjee, Silvia Naitza, Narisu Narisu, Matthew J Neville, Ben A Oostra, Marco Orrù, Ruth Pakyz, Colin N A Palmer, Giuseppe Paolisso, Cristian Pattaro, Daniel Pearson, John F Peden, Nancy L Pedersen, Markus Perola, Andreas F H Pfeiffer, Irene Pichler, Ozren Polasek, Danielle Posthuma, Simon C Potter, Anneli Pouta, Michael A Province, Bruce M Psaty, Wolfgang Rathmann, Nigel W Rayner, Kenneth Rice, Samuli Ripatti, Fernando Rivadeneira, Michael Roden, Olov Rolandsson, Annelli Sandbaek, Manjinder Sandhu, Serena Sanna, Avan Aihie Sayer, Paul Scheet, Laura J Scott, Udo Seedorf, Stephen J Sharp, Beverley Shields, Gunnar Sigurðsson, Eric J G Sijbrands, Angela Silveira, Laila Simpson, Andrew Singleton, Nicholas L Smith, Ulla Sovio, Amy Swift, Holly Syddall, Ann-Christine Syvänen, Toshiko Tanaka, Barbara Thorand, Jean Tichet, Anke Tönjes, Tiinamaija Tuomi, André G Uitterlinden, Ko Willems van Dijk, Mandy van Hoek, Dhiraj Varma, Sophie Visvikis-Siest, Veronique Vitart, Nicole Vogelzangs, Gérard Waeber, Peter J Wagner, Andrew Walley, G Bragi Walters, Kim L Ward, Hugh Watkins, Michael N Weedon, Sarah H Wild, Gonneke Willemsen, Jaqueline C M Witteman, John W G Yarnell, Eleftheria Zeggini, Diana Zelenika, Björn Zethelius, Guangju Zhai, Jing Hua Zhao, M Carola Zillikens, DIAGRAM Consortium, GIANT Consortium, Global BPgen Consortium, Ingrid B Borecki, Ruth J F Loos, Pierre Meneton, Patrik K E Magnusson, David M Nathan, Gordon H Williams, Andrew T Hattersley, Kaisa Silander, Veikko Salomaa, George Davey Smith, Stefan R Bornstein, Peter Schwarz, Joachim Spranger, Fredrik Karpe, Alan R Shuldiner, Cyrus Cooper, George V Dedoussis, Manuel Serrano-Ríos, Andrew D Morris, Lars Lind, Lyle J Palmer, Frank B Hu, Paul W Franks, Shah Ebrahim, Michael Marmot, W H Linda Kao, James S Pankow, Michael J Sampson, Johanna Kuusisto, Markku Laakso, Torben Hansen, Oluf Pedersen, Peter Paul Pramstaller, H Erich Wichmann, Thomas Illig, Igor Rudan, Alan F Wright, Michael Stumvoll, Harry Campbell, James F Wilson, Anders Hamsten on behalf of Procardis Consortium, Richard N Bergman, Thomas A Buchanan, Francis S Collins, Karen L Mohlke, Jaakko Tuomilehto, Timo T Valle, David Altshuler, Jerome I Rotter, David S Siscovick, Brenda W J H Penninx, Dorret I Boomsma, Panos Deloukas, Timothy D Spector, Timothy M Frayling, Luigi Ferrucci, Augustine Kong, Unnur Thorsteinsdottir, Kari Stefansson, Cornelia M van Duijn, Yurii S Aulchenko, Antonio Cao, Angelo Scuteri, David Schlessinger, Manuela Uda, Aimo Ruokonen, Marjo-Riitta Jarvelin, Dawn M Waterworth, Peter Vollenweider, Leena Peltonen, Vincent Mooser, Goncalo R Abecasis, Nicholas J Wareham, Robert Sladek, Philippe Froguel, Richard M Watanabe, James B Meigs, Leif Groop, Michael Boehnke, Mark I McCarthy, Jose C Florez & Inês Barroso for the MAGIC investigators

In the version of this article initially published, there were several errors in the author affiliations. These errors have been corrected in the HTML and PDF versions of the article.